

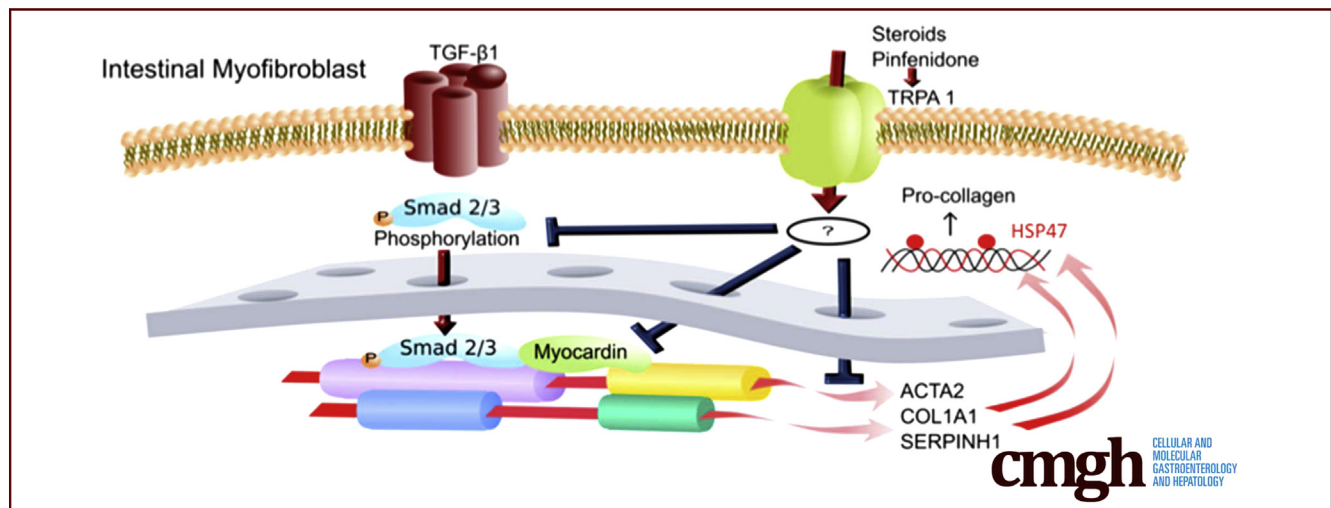
ORIGINAL RESEARCH

Activation of Myofibroblast TRPA1 by Steroids and Pirfenidone Ameliorates Fibrosis in Experimental Crohn's Disease



Lin Hai Kurahara,¹ Keizo Hiraishi,¹ Yaopeng Hu,¹ Kaori Koga,² Miki Onitsuka,² Mayumi Doi,^{1,3} Kunihiro Aoyagi,⁴ Hidetoshi Takedatsu,⁵ Daibo Kojima,⁶ Yoshitaka Fujihara,⁷ Yuwen Jian,⁸ and Ryuji Inoue¹

¹Department of Physiology, ²Department of Pathology, ⁵Department of Gastroenterology and Medicine, ⁶Department of Gastroenterological Surgery, Faculty of Medicine, Fukuoka University, Fukuoka, Japan; ³Department of Clinical Pharmacology and Therapeutics, Faculty of Medicine, Oita University, Oita, Japan; ⁴Department of Gastroenterology, Japanese Red Cross Fukuoka Hospital, Fukuoka, Japan; ⁷Research Institute for Microbial Diseases, Osaka University, Osaka, Japan; ⁸College of Letters and Science, University of California—Davis, Davis, California



SUMMARY

Steroids and pirfenidone activated the transient receptor potential ankyrin 1 (TRPA1) channel to inhibit fibrosis in vitro and in trinitrobenzene sulfonic acid colitis. TRPA1-positive cells accumulated within stenotic regions of Crohn's disease intestine. The results suggest that TRPA1 channel activation could be beneficial in fibrotic inflammatory disorders.

BACKGROUND & AIMS: The transient receptor potential ankyrin 1 (TRPA1) channel is highly expressed in the intestinal lamina propria, but its contribution to gut physiology/pathophysiology is unclear. Here, we evaluated the function of myofibroblast TRPA1 channels in intestinal remodeling.

METHODS: An intestinal myofibroblast cell line (InMyoFibs) was stimulated by transforming growth factor-β1 to induce in vitro fibrosis. *Trpa1* knockout mice were generated using the Clustered regularly interspaced short palindromic repeats (CRISPR)/CRISPR-associated 9 (Cas9) system. A murine chronic colitis model was established by weekly intrarectal trinitrobenzene sulfonic acid (TNBS) administration.

Samples from the intestines of Crohn's disease (CD) patients were used for pathologic staining and quantitative analyses.

RESULTS: In InMyoFibs, TRPA1 showed the highest expression among TRP family members. In TNBS chronic colitis model mice, the extents of inflammation and fibrotic changes were more prominent in TRPA1^{-/-} knockout than in wild-type mice. One-week enema administration of prednisolone suppressed fibrotic lesions in wild-type mice, but not in TRPA1 knockout mice. Steroids and pirfenidone induced Ca²⁺ influx in InMyoFibs, which was antagonized by the selective TRPA1 channel blocker HC-030031. Steroids and pirfenidone counteracted transforming growth factor-β1-induced expression of heat shock protein 47, type 1 collagen, and α-smooth muscle actin, and reduced Smad-2 phosphorylation and myocardin expression in InMyoFibs. In stenotic intestinal regions of CD patients, TRPA1 expression was increased significantly. TRPA1/heat shock protein 47 double-positive cells accumulated in the stenotic intestinal regions of both CD patients and TNBS-treated mice.

CONCLUSIONS: TRPA1, in addition to its anti-inflammatory actions, may protect against intestinal fibrosis, thus being a novel therapeutic target for highly incurable inflammatory/

fibrotic disorders. (*Cell Mol Gastroenterol Hepatol* 2018;5:299–318; <https://doi.org/10.1016/j.jcmgh.2017.12.005>)

Keywords: Crohn's Disease; Intestinal Fibrosis; Myofibroblast; Transient Receptor Potential Ankyrin 1.

Myofibroblasts play crucial roles in tissue repair and remodeling. The major profibrotic factor, transforming growth factor (TGF)- β , is secreted from many types of cells and is known to drive the transformation of fibroblasts to myofibroblasts. Activated myofibroblasts proliferate, migrate, and invade affected tissues to facilitate the formation of collagen-rich extracellular matrix and express α -smooth muscle actin (α -SMA) to confer contractility ability.^{1,2} We previously showed that cultured intestinal myofibroblasts (InMyoFibs) stimulated by TGF- β 1 actively secreted collagens to serve as an excessive fibrosis model. TGF- β 1 treatment induced characteristic morphologic changes in InMyoFibs, such as enlarged size and a filamentous microstructure.³ The activated TGF- β -receptor 1 complex has been shown to phosphorylate the transcription factors Smad-2 and Smad-3, which in turn promote collagen synthesis.⁴ TGF- β was reported to up-regulate heat shock protein 47 (HSP47), a collagen-specific molecular chaperone that plays a critical role in intestinal fibrosis. Blocking the bioactivities of HSP47 not only alters collagen production, but also reduces fibrotic lesions, directly implicating HSP47 in fibrogenesis.^{5,6} TGF- β modulates transcriptional regulation by the serum response factor and its cofactor myocardin-related transcription factor A during the induction of pathologic colonic myofibroblast differentiation.⁷

TGF- β levels are increased in inflamed intestines of patients with Crohn's disease (CD) and ulcerative colitis. However, TGF- β 1 also is essential for anti-inflammatory responses. Thus, the use of TGF- β 1-neutralizing antibodies for antifibrotic treatment in clinical practice may exacerbate CD progression by attenuating the anti-inflammatory actions of TGF- β 1. In addition, abnormal TGF- β signaling impairs intestinal immune tolerance and tissue repair.⁸


There is growing interest in the role of transient receptor potential (TRP) channels in the pathogenesis of tissue remodeling.^{9–12} We recently reported that transient receptor potential canonical (TRPC)4 and TRPC6 activities in myofibroblast are functionally linked to the progression of intestinal fibrotic stenosis.³ Our preliminary experiment indicated that another TRP member, TRP ankyrin 1 (TRPA1), is expressed abundantly at the messenger RNA (mRNA) level in intestinal myofibroblasts. TRPA1 is expressed in myenteric nerves and intestinal epithelial cells,^{13,14} and its activation has been shown to inhibit gut motility and protect against gut inflammation via an adrenomedullin-mediated increase in intestinal microcirculation.^{14–16} It also has been reported that a TRPA1 agonist allyl isothiocyanate (AITC) exerts anti-fibrogenic effects on hepatic stellate cells, and another TRPA1 agonist allicin prevents fibrotic changes in the oral submucosa and heart.^{17,18} Moreover, TRPA1 activity was reported to have anti-inflammatory actions on dextran sulfate sodium-induced chronic colitis.¹⁹ Given the chronic nature of

this colitis, T cells may contribute to its pathogenesis, with TRPA1 regulating the inflammatory potential of T cells. Indeed, genetic deletion of TRPA1 on an interleukin 10^{-/-} background exacerbated colitis, and TRPA1^{-/-} naive T cells were more colitogenic in a T-cell transfer model of colitis.²⁰ In contrast, TRPA1 activation by cannabichromene was found to reduce the severity of DNBS-induced colitis.²¹ However, the molecular mechanisms underlying these beneficial actions of TRPA1 activation remain largely unknown. One possible approach for answering these questions is to compare the severity of gastrointestinal inflammation/fibrosis between wild-type (WT) and TRPA1-deficient mice by developing colitis models.

In our ongoing project involving screening of 103 types of food ingredients, we identified 4 plant extract components with both TRPA1-activating and antifibrotic activities. These 4 components suppressed TGF- β 1-induced α -SMA and collagen production. Among them was the ethanol extract of licorice, which contains a steroid-like ingredient (glycyrrhizic acid). It is metabolized to glycyrrhetic acid and showed the strongest TRPA1-activating/antifibrotic activities. In clinical practice, steroids and pirfenidone are widely used antifibrotic drugs that target many organs, including intestinal strictures after surgical dilatation.^{22,23} These drugs also are known to mitigate inflammatory bowel disease-associated fibrosis and consequent stenosis and strictures, which are common and severe complications in CD patients.^{22–24} In many CD patients, surgery alone often results in only temporarily beneficial effects. Pirfenidone has been reported to suppress various types of fibrosis in animal models and was shown to be effective in clinical trials for patients with idiopathic pulmonary fibrosis. In the gastrointestinal tract, pirfenidone exerts antifibrotic effects by suppressing the expression of HSP47,²⁵ which acts as a collagen-specific molecular chaperone and participates in the intestinal fibrosis of CD.^{6,26,27}

In the present study, we examined whether myofibroblast TRPA1 is involved in the antifibrotic/antistenotic mechanisms in the intestine and whether steroids and pirfenidone exert their antifibrotic actions in the intestine by activating the myofibroblast TRPA1 channel. We prepared TRPA1-knockout mice and compared the *in vivo* results from mice with those of *in vitro* experiments using InMyoFibs. Moreover, biopsy samples from stenotic and

Abbreviations used in this paper: α -SMA, α smooth muscle actin; AITC, allyl isothiocyanate; CD, Crohn's disease; EGTA, ethylene glycol-bis(β -aminoethyl ether)-*N,N,N',N'*-tetraacetic acid; HSP47, heat shock protein 47; InMyoFib, intestinal myofibroblast cell line; KO, knockout; mRNA, messenger RNA; MT, Masson trichrome; PBS, phosphate-buffered saline; PCR, polymerase chain reaction; RT-PCR, reverse-transcription polymerase chain reaction; sgRNA, single-guide RNA; siRNA, small interfering RNA; TGF, transforming growth factor; TNBS, trinitrobenzene sulfonic acid; TNF, tumor necrosis factor; TRP, transient receptor potential; TRPA1, transient receptor potential ankyrin 1; TRPC, transient receptor potential canonical; WT, wild-type.

 Most current article

© 2018 The Authors. Published by Elsevier Inc. on behalf of the AGA Institute. This is an open access article under the CC BY-NC-ND license (<http://creativecommons.org/licenses/by-nc-nd/4.0/>).

2352-345X

<https://doi.org/10.1016/j.jcmgh.2017.12.005>

nonstenotic regions of intestines from CD patients were used to confirm the validity for human pathogenesis. Our results suggest that TRPA1 activity in myofibroblast cells negatively regulates TGF- β 1-induced α -SMA and collagen production, and thus direct stimulation of TRPA1 channels in the intestinal submucosa may be a promising intervention for relieving abdominal symptoms associated with intestinal fibrotic remodeling.

Materials and Methods

Materials

Licorice extract powder was dissolved in ethanol by sonication and purified by filtering. AITC and HC-030031 were obtained from Sigma-Aldrich (St. Louis, MO). Recombinant human TGF- β 1 (Wako, Osaka, Japan) was added to cultured cells according to the manufacturer's instructions. Human Stealth small interfering RNAs (siRNAs) for TRPA1 (TRPA1HSS113276 (5'-GGAGCAAUUGCUGUUUACUUCUAAUU-3' and 5'-AAUAGAAGUAAACAGCAAUUGCUC-3')) were obtained from Invitrogen (Carlsbad, CA) and used for gene silencing according to the manufacturer's instructions. Other TRPA1-siRNAs, TRPA1HSS113277 and TRPA1HSS189723, also were evaluated, but the silencing efficacy was inferior to that by TRPA1HSS113276 for InMyoFibs. Antibodies against TRPA1 (mouse, Sigma-Aldrich; rabbit, Novus, CO), HSP47 (rabbit; Abcam, Cambridge, UK), α -SMA (Abcam), β -actin (Abcam), collagen I (Abcam), Smad-2/3, and phospho-Smad-2 (Cell Signaling Technology, Danvers, MA) were used for immunoblotting and immunostaining experiments. The human TRPA1 plasmid used for single-channel recording was kindly provided by Professor Yasuo Mori (Kyoto University, Japan).

Cell Culture

Normal human InMyoFibs were purchased from Lonza (CC-2902; Basel, Switzerland) and grown in smooth muscle basal medium supplemented with 5% fetal bovine serum, antibiotics (gentamicin/amphotericin-B), and growth factors (insulin, human epidermal growth factor- β , and human fibroblastic growth factor). InMyoFibs cells were passaged 10–19 times. TGF- β 1 (5 ng/mL) was used under low-serum (1% fetal bovine serum) conditions.

Expression Array Analysis

Total RNA isolation for array. The total RNA was isolated from the InMyoFibs using TRIzol Reagent (Invitrogen) and purified using the SV Total RNA Isolation System (Promega, Madison, WI) according to the manufacturer's instructions. RNA samples were quantified using an ND-1000 spectrophotometer (NanoDrop Technologies, Wilmington, DE) and the quality was confirmed using an Experion System (Bio-Rad Laboratories, Hercules, CA).

Gene expression microarrays. The complementary RNA was amplified, labeled using a GeneChip (Affymetrix, CA) WT Terminal Labeling and Control Kit, and hybridized to an Affymetrix Human Genome U133 Plus 2.0 array according to the manufacturer's instructions. All hybridized microarrays were scanned with an Affymetrix scanner. Relative hybridization intensities and background hybridization values were calculated using the Affymetrix Expression Console.

Data analysis and filter criteria. Raw signal intensities for respective probes were calculated from hybridization intensities. Next, the raw signal intensities of 2 samples were log₂-transformed and normalized using the robust multi-array average and quantile algorithm with Affymetrix Expression Console 1.1 software. To identify up-regulated or down-regulated genes, we calculated Z-scores and ratios (non-log-scaled fold-change) from the normalized signal intensities of respective probes to compare control and experimental samples.

Electrophysiological Study

Whole-cell voltage clamp recording was conducted using an EPC-10 patch-clamp amplifier (HEKA Electronics, Lambrecht, Germany). Recording electrodes with resistances of 2–4 M Ω were pulled from glass capillaries. An Ag–AgCl wire was used as a reference electrode. Capacitive currents were compensated, and linear leak and residual capacitance were subtracted by the P/4 protocol. More than 70% series resistance was compensated to minimize voltage errors. Data analysis was performed offline using a versatile analysis software (Clampfit v.9.2; Axon Instruments, Union City, CA; and Origin 9.1; OriginLab Corporation, Northampton, MA). Long-term recordings were performed using an A/D, D/A converter PowerLab/400 (ADInstruments, Sydney, Australia; sampling rate, 100 Hz) and analyzed with the accessory software Chart v.5.0 (ADInstruments, Sydney, Australia). A solenoid valve-driven fast solution change device similar to the Y-tube system was used to rapidly apply drugs to the cells as described previously.²⁸ Membrane capacitance was measured to normalize current amplitudes and minimize the variance caused by differences in cell size. To obtain current density–voltage relationships, cells were held at a holding potential of -60 mV and then subjected to ramp pulses of 100 ms from -100 to 100 mV at a rate of 4 mV/ms. To prevent rapid Ca²⁺-dependent inactivation of TRPA1 currents, a Ca²⁺ chelator was added to both the bath solution and pipette solution.²⁹ The extracellular solution contained 140 mmol/L NaCl, 5 mmol/L KCl, 1 mmol/L MgCl₂, 5 mmol/L ethylene glycol-bis(β -aminoethyl ether)-N,N,N',N'-tetraacetic acid (EGTA), 10 mmol/L HEPES, and 10 mmol/L glucose. K⁺ currents were eliminated by adding Cs⁺ and tetraethylammonium (TEA) to the patch pipette solution. Patch pipettes were filled with 130 mmol/L Cs-aspartate, 10 mmol/L TEA-Cl, 5 mmol/L BAPTA, 1.374 mmol/L Ca-gluconate, 1 mmol/L MgCl₂, 2 mmol/L MgSO₄, 2 mmol/L Na₂ adenosine triphosphate, and 10 mmol/L HEPES. For cell-attached recording of expressed HEK293 cells, the pipette solution contained 140 mmol/L NaCl, 5 mmol/L KCl, 1 mmol/L MgCl₂, 5 mmol/L EGTA, 10 mmol/L HEPES, and 10 mmol/L glucose. The extracellular solution contained 145 KCl, 1.2 MgCl₂, 5 mmol/L EGTA, 10 mmol/L HEPES, and 10 mmol/L glucose.

Measurement of [Ca²⁺]_i

[Ca²⁺]_i in myofibroblasts was monitored using a digital fluorescence imaging technique with Fura-2. Briefly, InMyoFibs were dispersed onto a poly-L-lysine-coated (Sigma-Aldrich) glass chamber placed on the stage of an inverted

fluorescent microscope (DMI600B; Leica, Wetzlar, Germany). InMyoFibs cells then were loaded with 5 $\mu\text{mol/L}$ Fura-2/AM in the dark at 37°C for 30 minutes. The intensity of Fura-2 emissions at 510 nm (± 10 nm) resulting from excitation at 340 or 380 nm was measured using a fluorescent microscope (DMI600B) and a Cascade EMCCD camera (Nippon Roper, Tokyo, Japan). Data acquisition and analysis were performed using SlideBook 4.2 software (Intelligent Imaging Innovation, Inc, Denver, CO). Fluorescence intensities were corrected for background fluorescence and changes in $[\text{Ca}^{2+}]_i$ were defined as the ratio of corrected fluorescence intensities resulting from excitation at 340 and 380 nm (F_{340}/F_{380}). The normal external solution for Ca^{2+} -imaging experiments contained the following: 140 mmol/L NaCl, 5 mmol/L KCl, 1 mmol/L CaCl_2 , 1.2 mmol/L MgCl_2 , 10 mmol/L HEPES, and 10 mmol/L glucose (pH 7.4, adjusted with Tris base).

Immunoblot Analysis

Immunoblotting experiments were performed to examine the protein levels of type I collagen, α -SMA, β -actin, Smad-2/3, and phospho-Smad-2 in InMyoFibs as described previously. Total cell lysates were prepared in sample buffer and diluted in 5% (vol/vol) 2-mercaptoethanol and 1% (wt/vol) bromophenol blue before electrophoresis. Proteins were resolved on 10% (wt/vol) sodium dodecyl sulfate-polyacrylamide gels and transferred to polyvinylidene difluoride membranes. The membranes were blocked with Blocking One (Nacalai Tesque, Kyoto, Japan) and incubated overnight (4°C) with appropriate primary antibodies. Protein levels were detected by incubating the polyvinylidene difluoride membranes with appropriate species-specific, horseradish peroxidase-conjugated secondary antibodies (20°C, 45 min), and visualized using the ECL Western Blotting Detection System (GE Healthcare, Little Chalfont, UK).

Real-time Reverse-Transcription Polymerase Chain Reaction

Total RNA for quantitation was extracted from InMyoFibs, using the RNeasy RNA Extraction Kit (Qiagen,

Hilden, Germany). To quantify mRNA expression levels, real-time polymerase chain reaction (PCR) was performed using a BioMark HD System (Fluidigm, South San Francisco, CA). Thermocycling was performed using an initial denaturation at a hot start phase of 60 seconds at 95°C. This was followed by 35 cycles of 5 seconds at 96°C and 20 seconds at 60°C. The following TaqMan Gene Expression Assay kits from Life Technologies (Carlsbad, CA) were used for real-time PCR reactions: *TRPA1* (Hs00175798_m1, Mm01227437_m1), *MYOCD* (myocardin; Hs00538071_m1), *SERPINH1* (HSP47; Hs01060397_g1), *ACTA2* (α -SMA; Hs00426835_g1), and *COL1A1* (Hs00164004_m1).

Immunostaining

InMyoFibs cells and tissues and were fixed in 4% formaldehyde for 15 minutes and permeabilized with 0.3% Triton X-100 in the presence of 5% normal goat serum (Wako). Cells then were incubated overnight with primary antibodies (1:200 dilution) at 4°C, washed with phosphate-buffered saline (PBS), and incubated with an Alexa Fluor-conjugated secondary antibody (1:200 dilution; Life Technologies) for an additional 1 hour. Immunostained cells were analyzed using a Zeiss LSM 710 Confocal Microscope (Oberkochen, Germany). Images were acquired through a 40 \times objective lens, using default settings for pinhole width, laser intensity, and detector gain. 3,3'-Diaminobenzidine tetra hydrochloride staining was performed with the R.T.U.Vectastain Universal Elite ABCkit (Vector Lab, Inc, Burlingame, CA).

Generation of *Trpa1* Knockout Mice Using the CRISPR/Cas9 System

The validation of in vitro cleavage activity of single-guide RNA (sgRNA) and generation of knockout mice by pronuclear injection of the circular pX330 plasmid were performed as described previously.³⁰ Super-ovulated B6D2F1 female mice were briefly mated with B6D2F1 males and then fertilized eggs were collected. Circular pX330-sgRNA-S02 and

Table 1. Summary of the Profiles of CD Patients Whose Clinical Tissues Were Used to Compare Stenosis and Nonstenosis

Patient number	Age, y	Sex	Diagnosis	Stenosis area	Severity of stenosis	Clinical history	Past treatment	Sampling
01	22	M	CD, small and large intestine type	Sigmoid colon	Moderate	10	Anti-TNF α + AZA	Endoscopy
02	29	M	CD, small and large intestine type	Anastomosis	Moderate-severe	8	Anti-TNF α	Endoscopy
03	43	F	CD, small and large intestine type	Transverse colon	Moderate-severe	3	Anti-TNF α + AZA	Endoscopy
04	33	M	CD, large intestine type	Ascending colon	Moderate	8	Anti-TNF α	Endoscopy
05	51	M	CD, large intestine type	Descending colon	Moderate	5	Anti-TNF α	Endoscopy
06	40	M	CD, small and large intestine type	Sigmoid colon	Moderate-severe	15	Anti-TNF α	Endoscopy
07	49	M	CD, small and large intestine type	Sigmoid colon, anastomosis	Severe	26	Anti-TNF α	Surgery
08	51	M	CD, small and large intestine type	Ascending colon	Severe	24	TPN, Mesalazine	Surgery

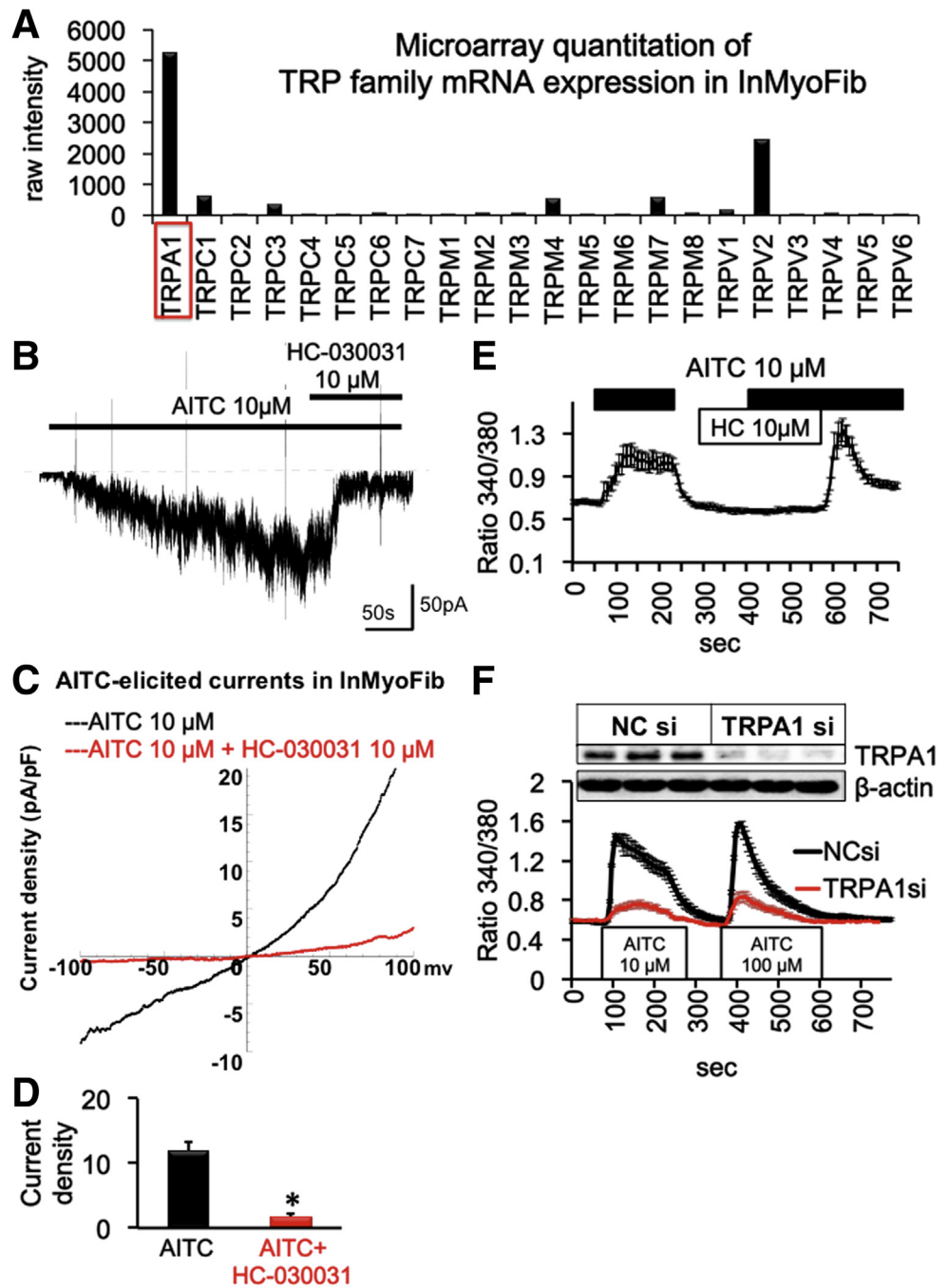
NOTE. Age, sex, diagnosis, stenosis area, severity of stenosis, clinical history, past main treatment, and sampling methods are listed. AZA, azathioprine; TPN, total parenteral nutrition.

pX330-sgRNA-AS02 plasmids targeting *Trpa1* were co-injected into the pronuclei of fertilized eggs. Off-target analysis was performed using Bowtie software (<http://bowtie-bio.sourceforge.net/index.shtml>).³¹ sgRNA sequences used for pX330 plasmid construction and injection were as follows: 5'-CAAT-GAAGCGCGGCTTGAGG-3' for sgRNA-S02 and 5'-CGCGCGGATA-GACAACGCC-3' for sgRNA-AS02. Primer sequences used for EGxxFP plasmid construction and genotyping were as follows: 5'-GCAGAGCTTAGTTGTAGGTCCTCAAGTCCGG-3' and 5'-TGATACTGTCTCCTGCCATTTCCATGTTCC-3'. Genotyping was performed by direct sequencing after PCR. Littermate mice generated from heterozygous crosses were used in the present study.

Trinitrobenzene Sulfonic Acid Chronic Colitis Model

Chronic trinitrobenzene sulfonic acid (TNBS)-associated colitis was induced as previously reported. Mice (ages, 8–9 wk; n = 8) were injected weekly with TNBS solution in 30% ethanol/PBS (10 mg/mL; 50 μ L) intracolonicly for 6 weeks. The vehicle group received 30% ethanol/PBS (50 μ L) for 6 weeks. Intracolonic administration was achieved after 24-hour fasting by inserting a polyethylene (PE10 Polyethylene; Braintree Scientific, Inc, Massachusetts) catheter 4 cm into the rectum under pentobarbital (40 mg/kg injected intraperitoneally with saline) anesthesia. Prednisolone was administered by enema for 1

Figure 1. (A) Microarray quantitation of TRP family mRNA expression and (B–D) electrophysiological characterization of TRPA1 currents in InMyoFibs cells. (B) Representative traces of whole-cell currents recorded from InMyoFibs cells at a holding potential of -60 mV. TRPA1 nonselective cation currents are activated by AITC (10 μ mol/L) and inhibited by HC-030031 (10 μ mol/L). (C) Current–voltage relationships of TRPA1 currents after application of AITC and HC-030031. (D) Peak current density of inward currents (-60 mV) after application of AITC and HC-030031 (n = 4) *P < .01. (E) Representative [Ca²⁺]_i responses in InMyoFibs cells. Cells were exposed to AITC (10 μ mol/L), and TRPA1 antagonist HC-030031 (10 μ mol/L) was added to examine whether Ca²⁺ influx is involved in TRPA1 channels. (F) Representative [Ca²⁺]_i responses in Negative control siRNA (NCsi) and TRPA1 siRNA (TRPA1si)-pretreated InMyoFibs cells. Knockdown of TRPA1 was confirmed by Western blot (upper panel). The vertical axis indicates the magnitude of Ca²⁺ influx expressed as the 340/380 fluorescence ratio. Data points represent the means \pm SEM from > 30 cells.



week (5 mg/kg/day; anesthetized by isoflurane) after the last TNBS treatment. Changes in body weight were monitored. Colonic tissues were excised from the anus to the cecum at week 6 after cervical dislocation. All animal experiments were conducted in accordance with the guidelines of the Animal Center of Fukuoka University.

Histologic Evaluation

The mouse distal colon samples and patient biopsy specimens were fixed in 10% buffered formalin, embedded in paraffin, and cut into 4- μ m-thick sections for routine H&E and Masson trichrome (MT) staining. Stained colon tissues were microphotographed at 200 \times magnification at 6 randomly chosen locations on each tissue and analyzed by a pathologist (K.K.) in a blinded manner. For all mice, the fibrosis score was measured at the tissue located 1 cm from the anus, where the most obvious fibrosis was observed. The optical density of blue-stained collagen fibers was measured and expressed as a fibrosis score on a scale of 0–3, as follows: 0, no fibrosis WT vehicle mouse; 1, mild fibrosis (focal mucosal/submucosal collagen deposition without architectural distortion); 2, moderate fibrosis

(significant mucosal/submucosal collagen deposition with modest distortion of mucosal/submucosal architecture but without obscuring the mucosal/submucosal border); and 3, severe fibrosis (extensive mucosal/submucosal collagen deposition with marked architectural distortion obscuring the mucosal/submucosal border).³²

Quantification of Fecal Lipocalin-2 by Enzyme-Linked Immunosorbent Assay

Fecal Lipocalin-2 (Lcn-2) levels were measured in WT and TRPA1-/- mice before TNBS treatment, TNBS 5 weeks (just before the last TNBS challenge), and TNBS 6 weeks (1 week after the last TNBS challenge), (n = 6–8). Freshly collected or frozen fecal samples were reconstituted in PBS containing 0.1% Tween 20 at a concentration of 100 mg feces/mL and vortexed for 20 minutes to yield a homogenous suspension. The samples were centrifuged at 12,000 rpm at 4°C for 10 minutes. Clear supernatant was collected and stored at -20°C until analysis. Lipocalin-2 levels were quantified using the Mouse Lipocalin-2/Neutrophil Gelatinase-associated Lipocalin (NGAL) enzyme-linked immunosorbent assay kit (R&D Systems, Minneapolis, MN).

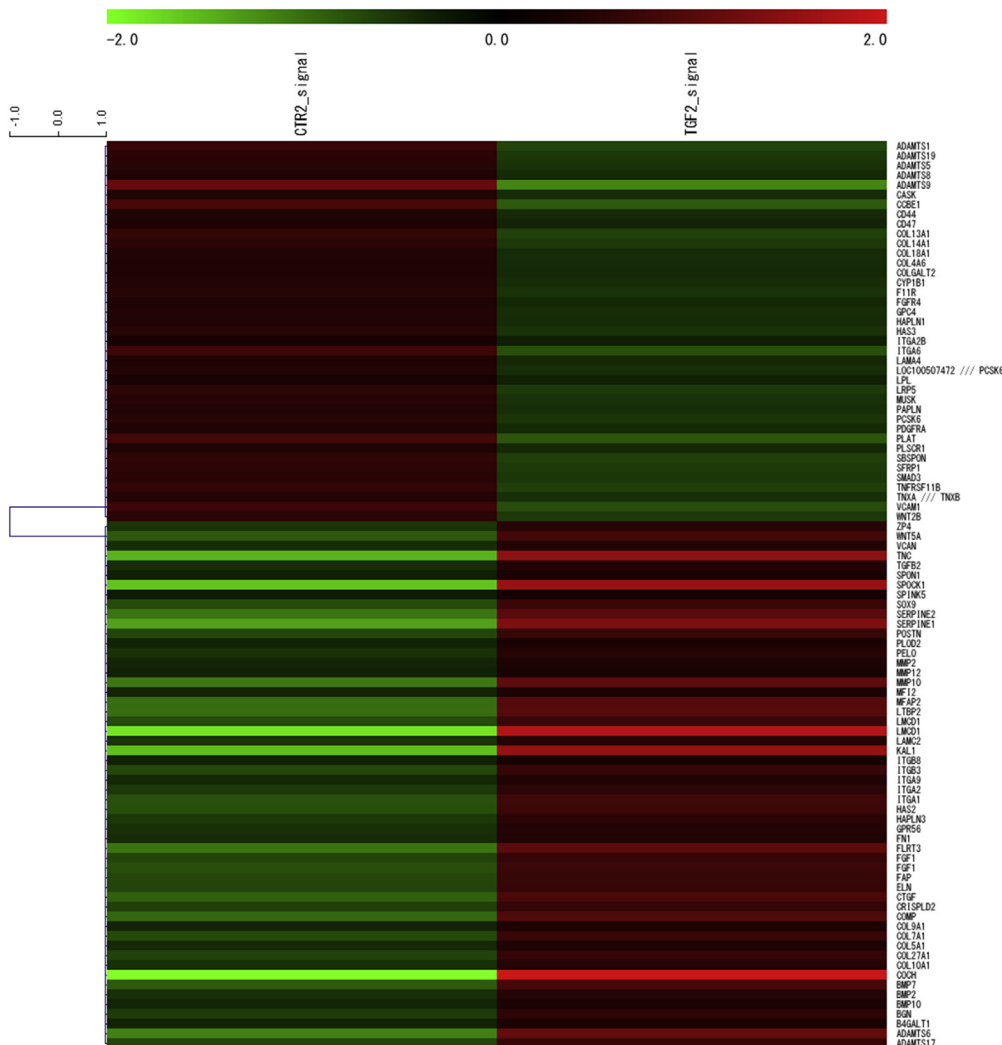


Figure 2. Fold-change heat map of fibrosis-associated molecule mRNAs in InMyoFibs by expression array analysis. Control vs TGF- β 1-treated (5 ng/mL, 24 h) InMyoFibs. The criteria for regulated genes were as follows: up-regulated genes, Z-score ≥ 2.0 and ratio ≥ 1.5 -fold; down-regulated genes, Z-score ≤ -2.0 and ratio ≤ 0.66 .

Patient Biopsy and Surgical Resected Tissues

As described previously,³ we studied biopsy samples from 8 CD patients with colonic lesions. The profiles of CD patients are summarized in Table 1. In all cases, the

patients had, in addition to co-existing stenosis, intra-abdominal or perianal fistula, and/or an abscess, during the disease course. Four patients had mucosal ulcerations, as determined by endoscopic evaluation. The Fukuoka

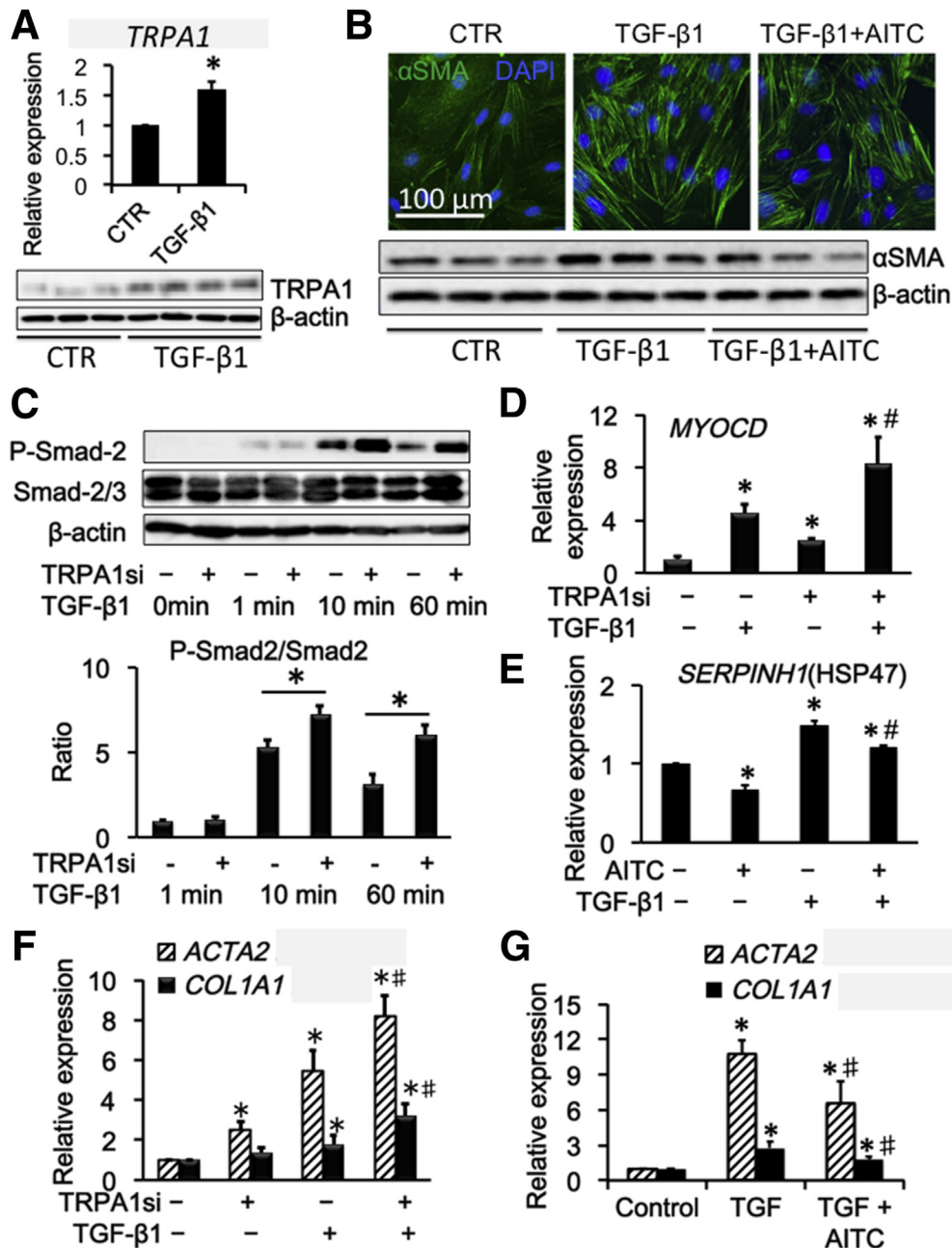


Figure 3. Antifibrotic drugs induced Ca^{2+} influx via TRPA1 in InMyoFibs. (A) Relative quantification of TRPA1/18S ribosomal RNA mRNA expression (upper panel) and Western blot (lower panel) of control (CTR) and TGF- β 1-stimulated (5 ng/mL, 24 h) InMyoFib cells. (B) Immunostaining images of InMyoFib cells stained with anti- α -SMA (green) antibody and 4',6-diamidino-2-phenylindole (DAPI) (blue) in untreated controls, after 24-hour TGF- β 1 (5 ng/mL) or TGF- β 1 (5 ng/mL)+AITC (10 μ mol/L) treatment (upper panel), and Western blot of α -SMA and β -actin were performed (lower panel). (C) TGF- β 1-induced phosphorylation of Smad-2 was measured by Western blot, with or without TRPA1-siRNA pretreatment. The ratios of phosphorylated/unphosphorylated Smad-2 proteins in TGF- β 1-treated cells are shown. (D and E) Myocardin (MYOCD) and HSP47 (SERPINH1) mRNA expression by real-time PCR in Negative control siRNA (NCsi) and TRPA1 siRNA (TRPA1si)-pretreated InMyoFib cells. (F) Relative quantitation of COL1A1 and ACTA2 mRNA expression by real-time PCR in NCsi and TRPA1si-pretreated InMyoFib cells. (G) Relative quantitation of COL1A1 and ACTA2 mRNA expression, AITC (10 μ mol/L) was co-administered with TGF- β 1. * P < .05 vs control cells; # P < .05 vs TGF- β 1-treated cells (n = 4).

University Hospital Ethics Committee approved the protocol, and written informed consent was obtained from all patients. After undergoing colonoscopies, 2 paired biopsy samples were obtained from each patient, 1 from stenotic areas and the other from nonstenotic areas 3 cm away from each stenotic area. Biopsy samples and surgically resected tissues for histologic evaluation were fixed in 10% buffered formalin. Samples for RNA quantitation were stabilized in RNAlater solution (Life Technologies) and homogenized for total RNA isolation. TaqMan real-time reverse-transcription PCR (RT-PCR) was performed on these samples ($n = 8$).³

Statistical Analysis

The results of electrophysiological study, quantitative PCR, Western blot, and $[Ca^{2+}]_i$ measurement are expressed as the means \pm SEM. Experimental protocols were repeated with at least 4 different batches of cells under each condition, and pooled data were averaged and subjected to statistical analyses. Statistically significant differences among groups were evaluated by analysis of variance (1-way and 2-way analysis of variance), and the Dunnett test was used for multiple comparisons where appropriate. P values $<.05$ were considered statistically significant.

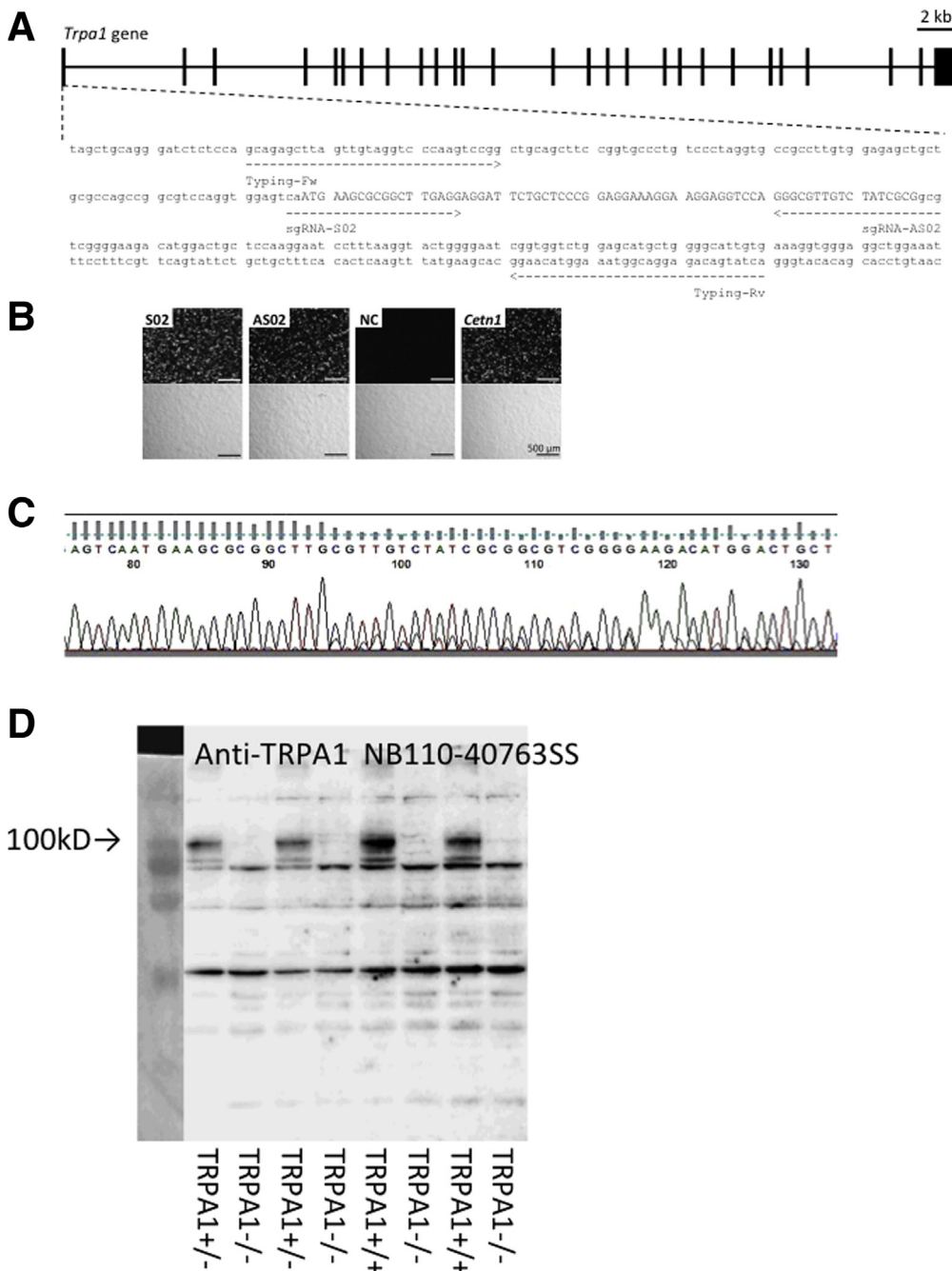


Figure 4. CRISPR/Cas9-mediated *Trpa1* gene mutation. (A) Complex of CAS9 and sgRNAs, S02 and AS02, recognized exon 1 of *Trpa1* and induced genomic mutations. Indels introduced by the sgRNA/CAS9-expressing plasmid (pX330) were identified by PCR using the primer set, typing forward and reverse. The region of capital letters indicates the coding region of *Trpa1*. (B) The pCAG-EGFP-*Trpa1* plasmid was co-transfected with pX330 plasmids containing sgRNA sequences, S02 and AS02, into HEK293T cells. Reconstituted enhanced green fluorescent protein (EGFP) fluorescence was observed at 48 hours after transfection. Fluorescence intensity was compared with the pCAG-EGFP-*Trpa1* and pX330 without sgRNA as the positive control. Transfection of pCAG-EGFP-*Trpa1* and pX330 without sgRNA was used as the negative control (NC). Generation of *Trpa1* mutant mice was injected with the circular pX330 plasmid with sgRNA-S02 and sgRNA-AS02. (C) Genotype of *Trpa1* mutant mice by sequence analysis. Raw data of DNA sequence of TRPA1^{+/-} mouse is shown. (D) TRPA1 knockout was analyzed by Western blot using anti-TRPA1 antibody NB110-40763SS.

Results

Functional Expression of TRPA1 Channel in InMyoFibs

Microarray quantitation of InMyoFibs indicated that the mRNA level of TRPA1 was highest among TRP family members (Figures 1A and 2). Consistent with this result, whole-cell patch clamp experiments showed robust induction of a nonselective cation current in response to the potent TRPA1 agonist AITC (10 μmol/L) in InMyoFibs (Figure 1B). The AITC-induced current showed typical features of TRPA1 channel, that is, prominent outward rectification (Figure 1C) and potent blockade by the TRPA1-selective antagonist HC-030031 (10 μmol/L) (Figure 1D). The same concentration of this compound nearly completely suppressed the intracellular Ca²⁺ increase ([Ca²⁺]_i) elicited by AITC (Figure 1E). To further

confirm that the responses induced by AITC represented TRPA1 channel activities, we specifically knocked down TRPA1 in InMyoFibs, using an siRNA strategy. As shown in Figure 1F, 24-hour treatment with TRPA1-targeting siRNA in InMyoFibs resulted in substantial elimination of TRPA1 protein expression as well as AITC-induced [Ca²⁺]_i increase. These results indicate that InMyoFibs express functional TRPA1 channels that permeate Ca²⁺.

TRPA1 Channel Activation Attenuates TGF-β1-Induced Stress-Fiber Formation and Collagen Synthesis

We then explored the possible contribution of TRPA1 to fibrotic changes induced by TGF-β1 treatment. Twenty-four-hour treatment of InMyoFibs with 5 ng/mL TGF-β1 enhanced the expression of TRPA1 mRNA and protein

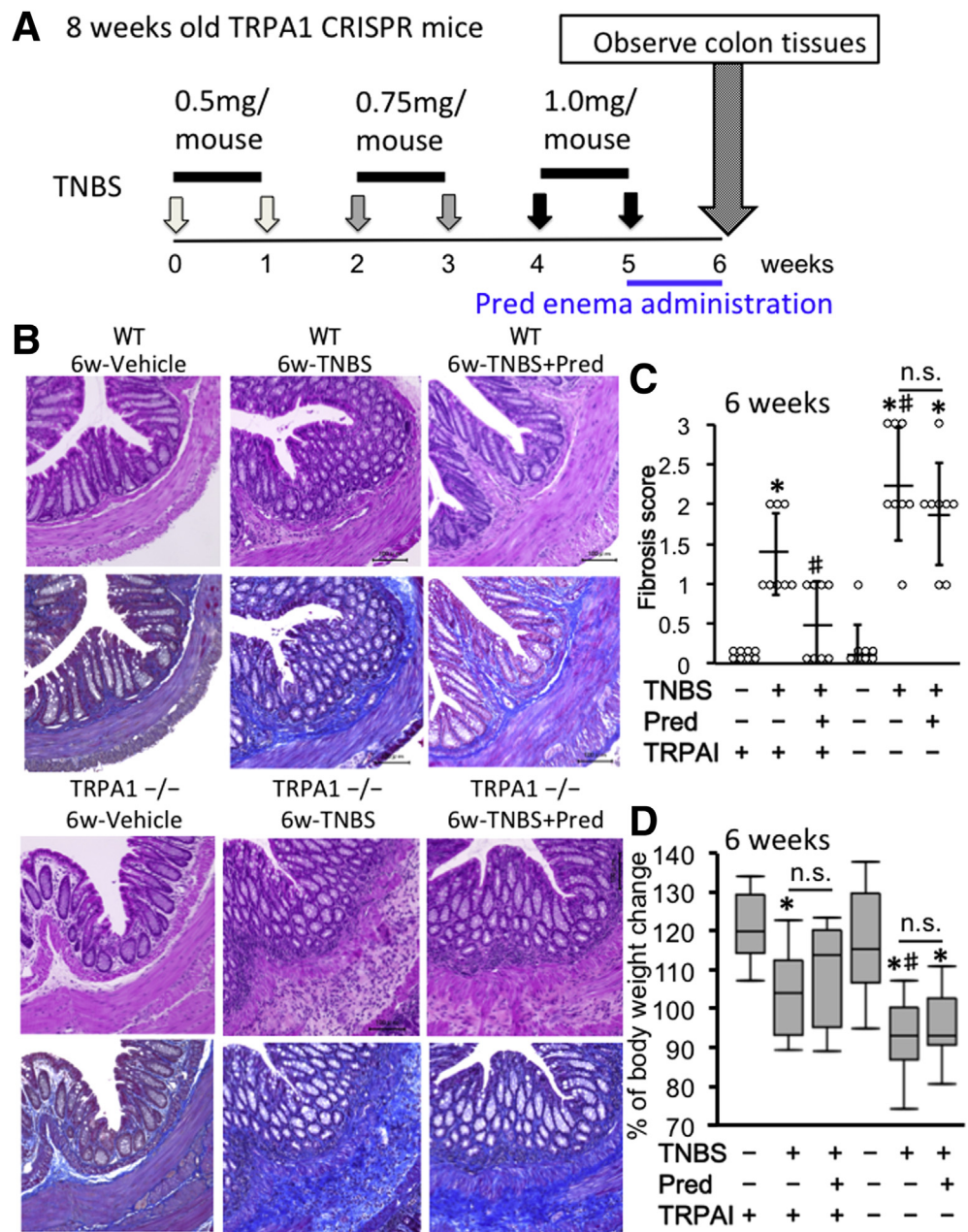


Figure 5. Validation of chronic TNBS-induced colitis in WT and TRPA1^{-/-} CRISPR mouse. Chronic colitis was induced by weekly intrarectal injection of TNBS for 6 weeks. (A) TNBS injection scheme. (B) H&E- and MT-stained tissues in vehicle, TNBS, and TNBS+Prednisolone (Pred) groups of WT and TRPA1^{-/-} mice. In the TNBS sections, chronic active inflammation and fibrosis. (C) Histologic fibrosis score from 0 (no fibrosis) to 3 (severe fibrosis) was shown in dot plot graph. The leftmost circles (n = 8) show absolutely zero values. Values are the means ± SD. (D) Body weight change in each experimental group was shown in box plot graph. *P < .01 vs WT vehicle; #P < 0.01 vs WT TNBS (n = 8).

(Figure 3A). Concomitantly, TGF- β 1 facilitated stress fiber formation and protein expression of α -SMA, which were suppressed effectively by co-treatment with 10 μ mol/L AITC (Figure 3B). Analyses of the downstream cascade of TGF- β 1-mediated signaling showed that increased mRNA expression of the master transcription regulator *MYOCD* by TGF- β 1 was enhanced further by TRPA1 knockdown, with increased phosphorylation of Smad-2 (Figure 3C and D). In addition, TRPA1 agonist AITC effectively suppressed the up-regulation of HSP47 by TGF- β 1 (Figure 3E). siRNA knockdown of TRPA1 enhanced the expression of α -SMA (*ACTA2*) and collagen type 1A1 (*COL1A1*) both in the presence and absence of TGF- β 1 (Figure 3F). TGF- β 1 treatment also increased the mRNA expression of *ACTA2* and *COL1A1*, which were antagonized by AITC (Figure 3G). These results collectively suggest that TRPA1 activity negatively regulates TGF- β 1-mediated, fibrosis-associated signaling in InMyoFibs.

Chronic TNBS Fibrosis Model of TRPA1-Knockout Mice

The *Trpa1* knockout (KO) mice were generated by the CRISPR/Cas9 system (Figure 4). Chronic colitis was induced by repeated administration of TNBS over 6 weeks (Figure 5A). TNBS is known to be more suitable than dextran sulfate sodium for investigating the pathogenesis of fibrosis in inflammatory bowel disease because the former has been found to cause much slower and more moderate progression of gut inflammation and fibrosis in mouse colitis models.^{33,34}

At 6 weeks of TNBS treatment, as compared with WT mice, TRPA1-KO mice treated with TNBS showed severer signs of inflammation/fibrosis characterized by prominent cell infiltration in some mucosal and submucosal layers and lower body weight increase (Figure 5B–D). To assess the total inflammation level, we quantified fecal lipocalin-2 by enzyme-linked immunosorbent assay (Figure 6A). The level of fecal lipocalin-2 significantly increased by repeated TNBS administration. At 5 and 6 weeks of TNBS administration when fibrosis occurred mildly and moderately/severely, respectively, increases in fecal lipocalin-2 level by TNBS treatment were not statistically different between WT and TRPA1-KO mice by 2-way analysis of variance. In TRPA1-KO mice treated with TNBS for 6 weeks, mucosal destruction was occasionally observed in a few parts of severely inflamed areas of intestine (Figure 6B).

At 5 weeks of TNBS treatment (just before prednisolone administration), no statistically significant differences could be detected in the extent of fibrosis among WT and TRPA1-KO mice (Figures 6C and 7), probably because of mild and slow progression of fibrotic changes. However, after 6 weeks, fibrosis scores assessed by histopathologic examination were significantly higher in TRPA1-KO than in WT mice ($P < .01$ for both) (Figure 5B and C), with pronounced extension of collagen fibers into the submucosal layer (Figures 5B and 6B). Just after the final TNBS treatment (ie, at 5 weeks TNBS treatment), we administered a prednisolone enema for 1 week. With this procedure, the fibrosis

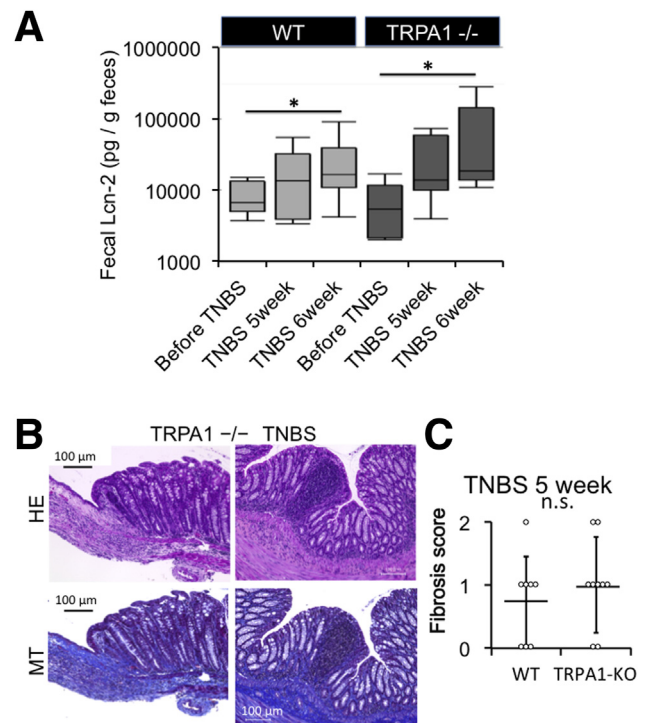


Figure 6. Support data of inflammation and fibrosis. (A) Box plots of fecal lipocalin-2 level quantified using an enzyme-linked immunosorbent assay kit. Fecal lipocalin (Lcn-2) levels were measured before and 5 or 6 weeks after TNBS administration, in WT mouse and TRPA1^{-/-} mouse before TNBS treatment. TNBS 5 weeks (just before last treatment), TNBS 6 weeks, respectively. By using 2-way analysis of variance with TNBS treatment and TRPA1 knockout as 2 independent variables, only the former turned out to be a statistically significant factor ($*P < .05$, $n = 6-8$). (B) Severe inflammation and fibrosis in TNBS-treated TRPA1-CRISPR knockout mouse. H&E-stained and MT-stained TRPA1^{-/-} CRISPR mouse intestine. (C) Histologic fibrosis score from 0 (no fibrosis) to 3 (severe fibrosis) of WT and TRPA1^{-/-} mouse before last TNBS challenge (TNBS 5 weeks) was shown in dot plot graph ($n = 8$). Values are means \pm SD.

score was remarkably reduced in WT mice, whereas no change was observed in TRPA1 KO mice (Figure 5B and C). Overall views of MT staining at 1–4 cm from the anus of vehicle- or TNBS-treated mice (vehicle 6 weeks, TNBS 5 weeks and 6 weeks) are shown in Figure 7. These observations strongly suggest that TRPA1 channel activity is crucial for counteracting the inflammatory/fibrogenic responses in chronic colitis.

Double-immunostaining experiments indicated a high co-occurrence of immunoreactivities against TRPA1 and HSP47, an endoplasmic reticulum-resident molecule essential for correct procollagen folding (Figure 8A and B). TNBS treatment significantly increased the expression level of TRPA1 mRNA in wild-type mouse colons ($P < .05$ for TNBS vs vehicle group) (Figure 8C). The number of TRPA1/HSP47 double-positive cells per unit area greatly increased in the TNBS-treated group compared with in the vehicle groups (Figure 8D). The protein level of TRPA1 was significantly up-regulated by TNBS treatment (Figure 8E).

Steroids and Pirfenidone Induce Ca^{2+} Influx via TRPA1 and Suppress Collagen Synthesis in InMyoFibs

In our ongoing project involving screening 103 types of food ingredients, we identified that the steroid-like active principle of licorice (glycyrrhetic acid) has antifibrotic activity in InMyoFibs (see Introduction). As described earlier, steroids and pirfenidone are widely used antifibrotic drugs for various fibrotic diseases. We therefore hypothesized that the antifibrotic effects of these compounds may in part involve activation of the TRPA1 channel. To test this hypothesis, we first examined the Ca^{2+} -mobilizing effects of these molecules on InMyoFibs.

As shown in Figures 9B, 10A, 11A, 11B, and 12A, licorice, and its active principle glycyrrhetic acid, and steroids methylprednisolone, prednisolone, and pirfenidone, all evoked robust $[Ca^{2+}]_i$ increases in InMyoFibs. These $[Ca^{2+}]_i$ increases were comparable in magnitude with that evoked by 10 $\mu\text{mol/L}$ AITC (Figure 1E), and were completely inhibited by prior application of the TRPA1-selective antagonist HC-03001, suggesting that the Ca^{2+} -mobilizing effects of these compounds are mediated by TRPA1 channel activation. Application of methylprednisolone (100 $\mu\text{mol/L}$) and AITC (5 $\mu\text{mol/L}$) to HEK293 cells expressing TRPA1 also induced TRPA1 channel activities in the cell-attached patch clamp recording (membrane potential $[V_m = -40 \text{ mV}]$) (Figure 11C).

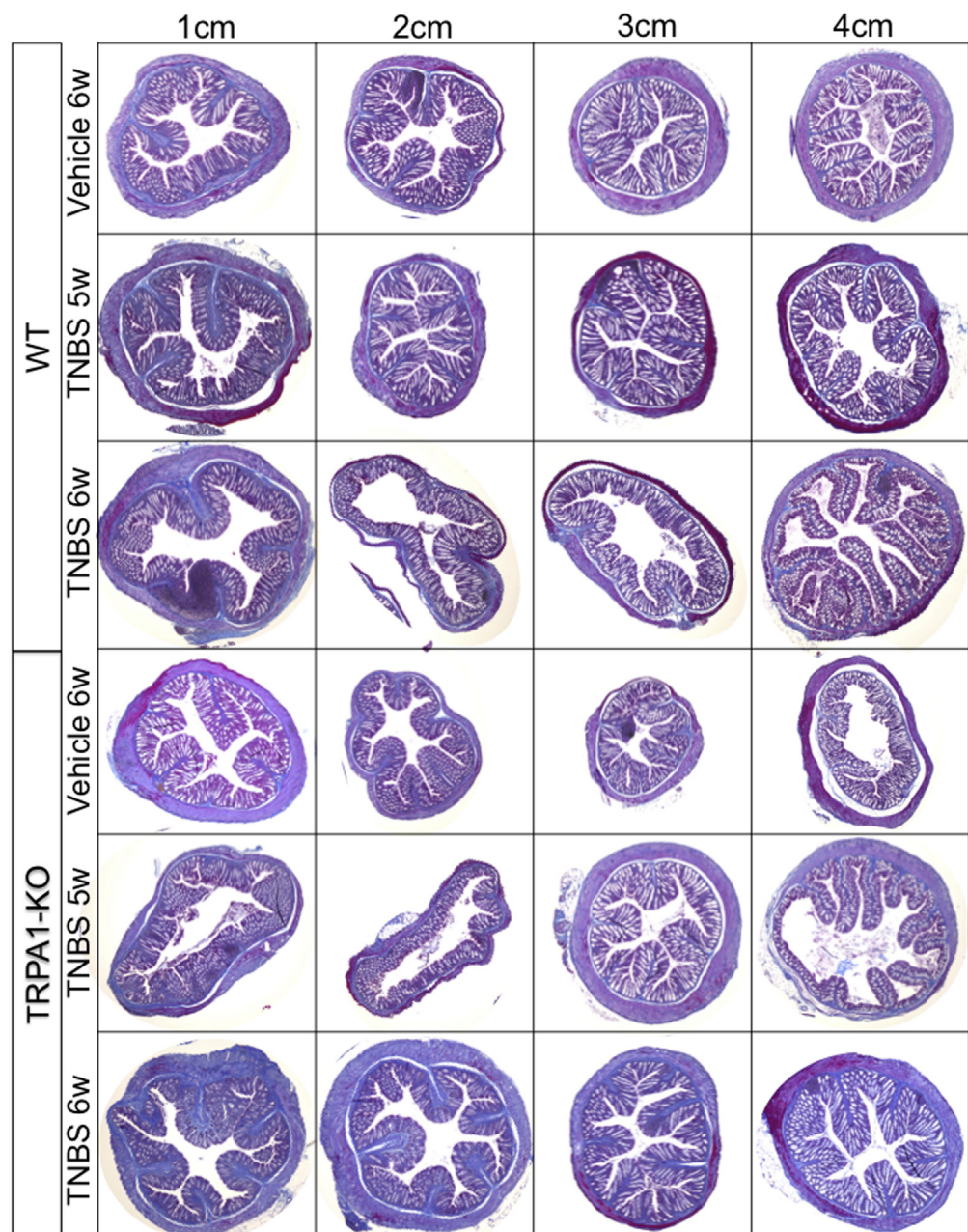


Figure 7. An overall view of MT staining of 1 cm, 2 cm, 3 cm, and 4 cm from the anus of the vehicle mouse or TNBS mouse is shown. Evaluation of fibrosis was performed with a stained image 1 cm from the anus.

We found that the traditional herbal medicine licorice can activate the TRPA1 channel and inhibit TGF- β 1-induced α -SMA and type 1 collagen production (Figure 9D and E). In real-time RT-PCR analyses of InMyoFibs, glycyrrhetic acid, prednisolone, and pirfenidone dose-dependently inhibited the enhanced mRNA expression of *ACTA2* and *COL1A1* by TGF- β 1 (Figures 10D, 10E, 11G, 11H, 12E, and 12F). The maximum extent of this inhibition was similar to that produced by AITC (Figure 3G). Importantly, these inhibitory effects of prednisolone, pirfenidone, glycyrrhetic acid, and AITC were well-correlated with suppression of Smad-2 phosphorylation and HSP47 and *MYOCD* expression induced by TGF- β 1 treatment (Figures 3C-E, 10B and C, 11D-F, and 12B-D). However, in TRPA1-siRNA-treated InMyoFibs, the enhanced mRNA expression of *COL1A1* and *ACTA2* by TGF- β 1 were no longer suppressed by prednisolone and pirfenidone (Figure 12G and H).

Enhanced TRPA1 Expression in Stenotic Tissues of CD Patients

Because intestinal stricture formation in CD is driven by local excessive accumulation of myfibroblasts,^{2,35} we examined whether TRPA1 is up-regulated in highly fibrotic areas of human CD patients. Biopsy samples obtained from the patients' intestines were subjected to histologic examination, immunostaining, and real-time RT-PCR to detect fibrosis-associated molecules. Histologic examination with H&E and MT staining showed much denser deposition of collagen fibers in the mucosal layer of the fibrotic stenotic area compared with in the nonstenotic area (Figure 13A). Moreover, double-immunostaining of biopsy tissues showed that the number of TRPA1/HSP47 double-positive cells in the mucosal layer of the stenotic area appeared larger than that in the nonstenotic area (Figure 13B). As summarized in Figure 13C, the mRNA expression of *TRPA1* and *HSP47* were significantly enhanced in

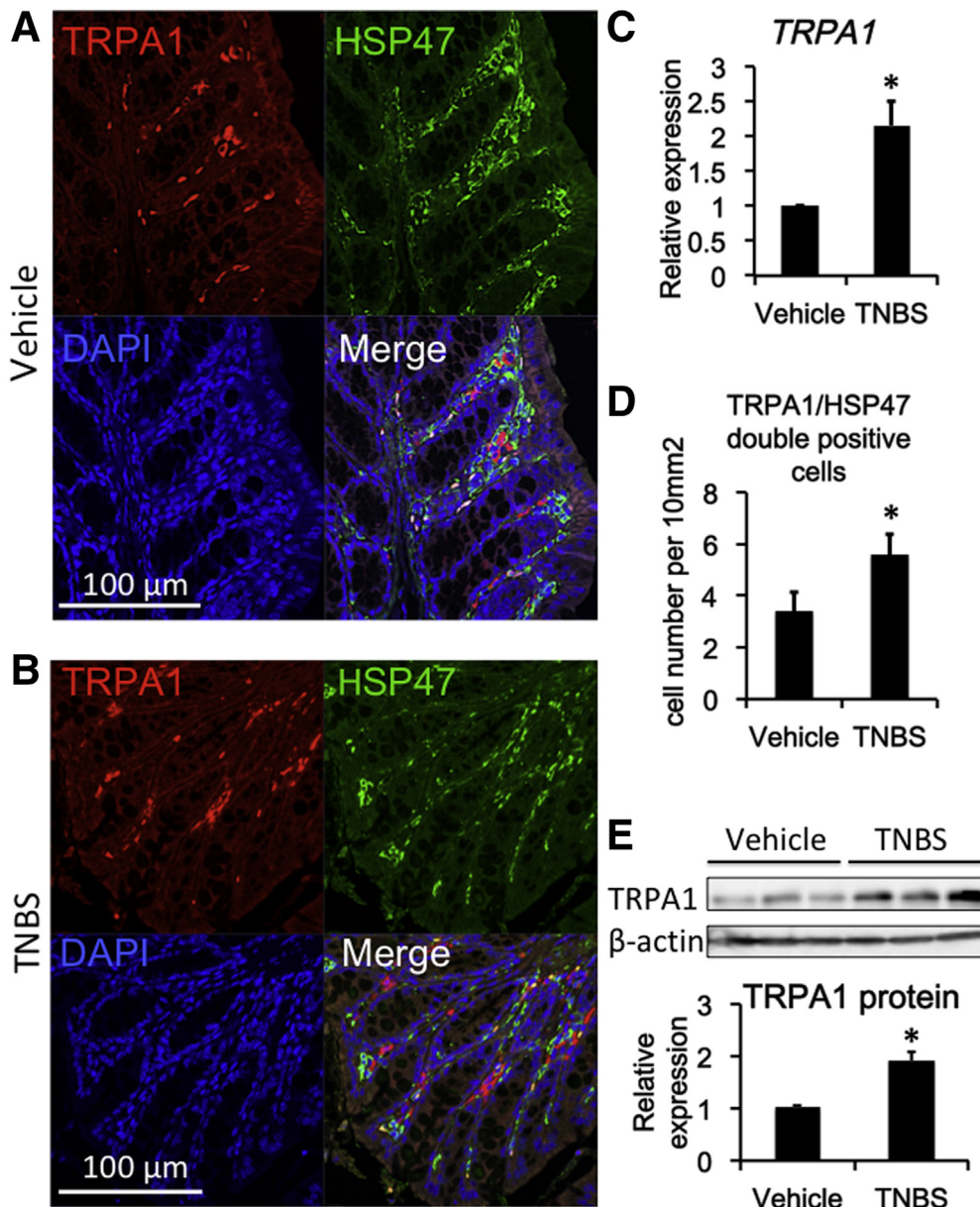


Figure 8. Co-localization of TRPA1 channel and HSP47 in mouse intestine. (A) Vehicle, (B) TNBS: Immunostaining images of mouse intestine stained with anti-TRPA1 (red) antibody, anti-HSP47 (green), and 4',6-diamidino-2-phenylindole (DAPI) (blue). (C) TRPA1 mRNA expression in vehicle and TNBS-treated colitis mouse ($n = 5$). (D) Number of TRPA1/HSP47 double-positive cells per unit area: 10 mm^3 counted from immunostaining data ($n = 5$). (E) Western blot analysis of TRPA1 and β -actin in WT vehicle and WT TNBS mouse distal colon ($n = 5$). * $P < .05$ vs vehicle.

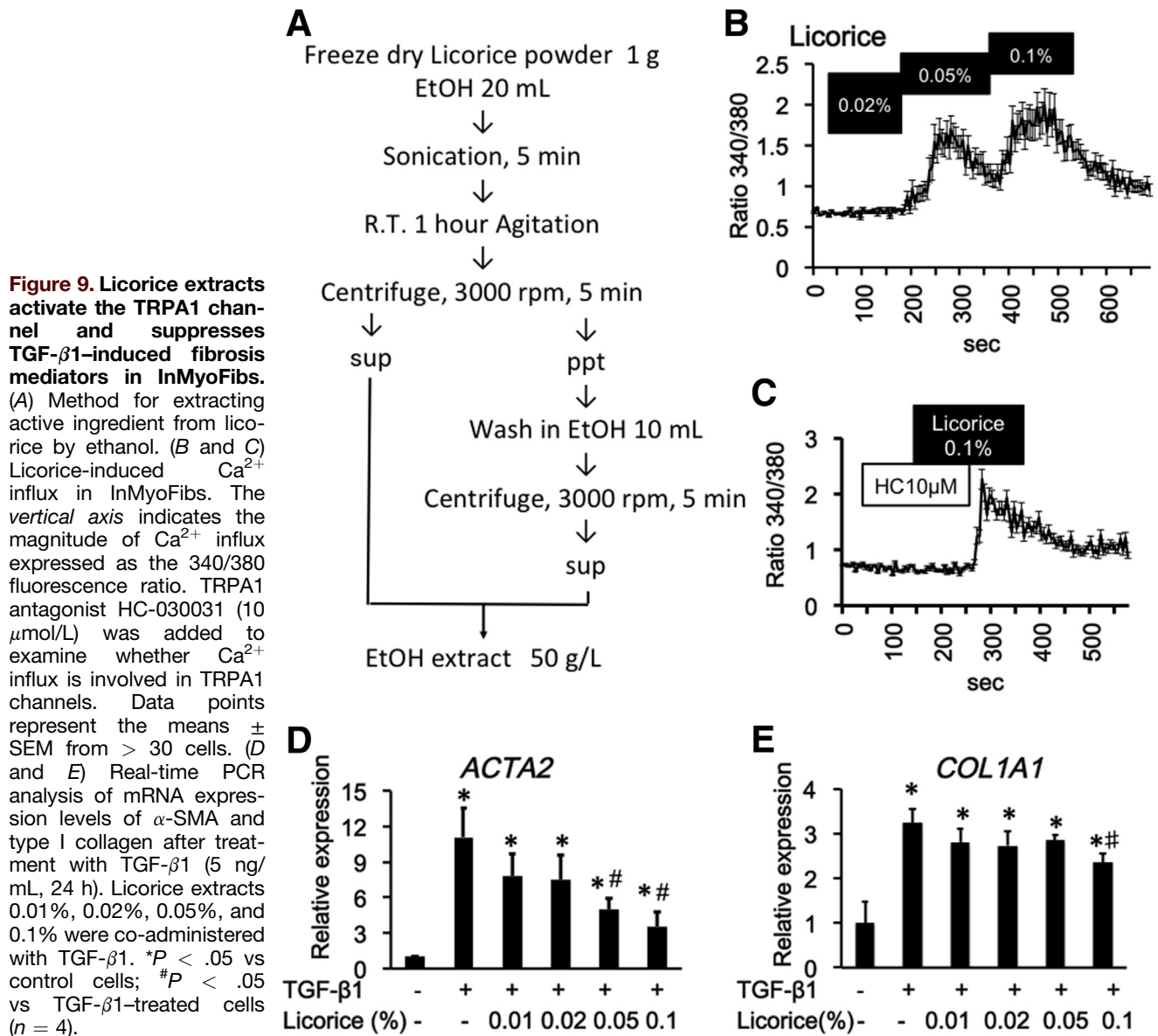


Figure 9. Licorice extracts activate the TRPA1 channel and suppresses TGF- β 1-induced fibrosis mediators in InMyoFibs. (A) Method for extracting active ingredient from licorice by ethanol. (B and C) Licorice-induced Ca^{2+} influx in InMyoFibs. The vertical axis indicates the magnitude of Ca^{2+} influx expressed as the 340/380 fluorescence ratio. TRPA1 antagonist HC-030031 (10 $\mu\text{mol/L}$) was added to examine whether Ca^{2+} influx is involved in TRPA1 channels. Data points represent the means \pm SEM from > 30 cells. (D and E) Real-time PCR analysis of mRNA expression levels of α -SMA and type I collagen after treatment with TGF- β 1 (5 ng/mL, 24 h). Licorice extracts 0.01%, 0.02%, 0.05%, and 0.1% were co-administered with TGF- β 1. * $P < .05$ vs control cells; # $P < .05$ vs TGF- β 1-treated cells ($n = 4$).

stenotic compared with nonstenotic regions. In agreement with this, the mRNA levels of fibrosis factors, that is, *ACTA2*, *CDH2*, *COL1A1*, *COL3A1*, matrix metalloproteinase 1 (*MMP1*), *MMP2*, tissue inhibitor of metalloproteinase 1, and tissue inhibitor of metalloproteinase 2 were much higher in stenotic than nonstenotic areas of CD patients (Figure 13C).³ Increased mRNA and protein expression of *TRPA1* and *SERPINH1* (HSP47) in the stenotic area was observed (Figure 13D). TRPA1/ α -SMA double-positive cells suggested TRPA1 expressed intestinal myofibroblast (Figure 14A); TRPA1 signals detected by 3,3'-diaminobenzidine tetra hydrochloride staining were distributed more diffusely in the mucosal and submucosal layers of stenotic regions in the intestines of CD patients (Figure 14B).

Discussion

Activation of TGF- β -mediated signaling pathways underlies the stenotic complications of CD patients. However,

simple neutralizing therapy targeting this signaling is not beneficial and can even exacerbate the inflammatory response.⁸ In this respect, the present study provides 2 novel and clinically important insights. First, in both in vitro and in vivo experiments as well as in human biopsy sample examination, the obtained evidence strongly supports that increased activity of TRPA1 channels in myofibroblasts protects against intestinal fibrogenesis. Second, we found that TRPA1 channel activation underlies the antifibrotic effects of steroids, pirfenidone, and licorice (and its active principle glycyrrhetic acid). These conclusions are supported by several different observations. First, TRPA1 mRNA was highly expressed in myofibroblasts and remarkably up-regulated in stenotic regions of human CD patient intestines. Second, TNBS-treated mice showed stromal fibrosis in the mucosal and submucosal layers of colon with active inflammatory cell infiltration. Fibrosis scores assessed by using this colitis model were significantly

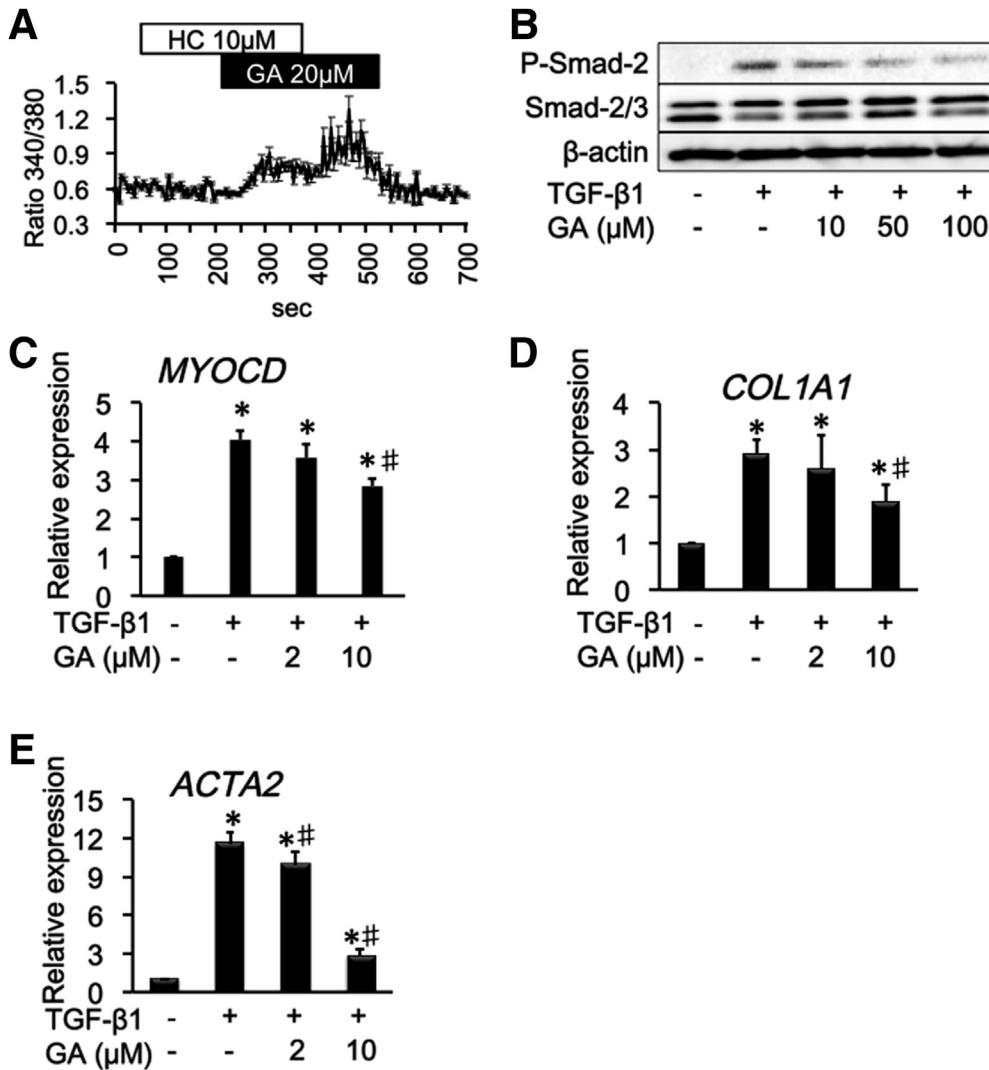


Figure 10. Glycyrrhetic acid (GA) activates the TRPA1 channel and suppresses TGF- β 1-induced fibrosis mediators in InMyoFibs. (A) GA induced Ca^{2+} influx in InMyoFibs. The vertical axis indicates the magnitude of Ca^{2+} influx expressed as the 340/380 fluorescence ratio. TRPA1 antagonist HC-030031 (10 μ mol/L) was added to examine whether Ca^{2+} influx is involved in TRPA1 channels. Data points represent the means \pm SEM from > 30 cells. (B) TGF- β 1-induced phosphorylation of Smad-2 was measured by Western blot, with or without GA pretreatment. (C–E) Real-time PCR analysis of mRNA expression levels of MYOCD, α -SMA, and type I collagen after treatment with TGF- β 1 (5 ng/mL, 24 h). GA was co-administered with TGF- β 1. * $P < .05$ vs control cells; # $P < .05$ vs TGF- β 1-treated cells ($n = 4$).

higher in TRPA1-KO mice compared with wild-type mice, and 1-week prednisolone treatment after the last TNBS administration suppressed fibrosis changes only in wild-type mice. Third, pirfenidone and steroids were able to elicit Ca^{2+} influx via TRPA1 channel activation with comparable efficacies to the TRPA1-selective agonist AITC. These compounds also counteracted TGF- β -induced fibrotic changes (ie, reduced the expression of fibrosis markers) and suppressed HSP47 expression in InMyoFibs. Fourth, TRPA1/HSP47 double-positive cells accumulated in the submucosal layer of intestines of both CD patients and TNBS mice. In the stenotic area of CD patients, many cells were doubly immunopositive for TRPA1 and HSP47 in the submucosal layer, where numerous collagen fibers were stained and fibrosis markers were significantly up-regulated. Notably, both TRPA1 and HSP47 are known to be activated not only by temperature increases, but also by many other physicochemical stimuli. Overall, these findings support the antifibrotic actions of steroids, pirfenidone, and possibly licorice or its active principle glycyrrhetic acid in

intestinal myofibroblasts and indicate their therapeutic potential for CD-associated intestinal stenosis.

However, TRPA1 channel activation in the digestive tract clearly causes anti-inflammatory actions by modifying immune responses. Bertin et al²⁰ reported that TRPV1-mediated CD4^{+} -T-cell activation and the resultant colitogenic response were restrained by TRPA1 activity in the same cell, ultimately retarding fibrotic processes. Although this mechanism may have affected our experiments to some extent, the results of the present study clearly showed an additional mechanism operating through myofibroblast TRPA1 activation. This mechanism prevents fibrogenesis during the sustained phase of inflammatory colitis, as indicated by the fact that steroids introduced in the fifth week of the 6-week TNBS administration protocol (which should have already developed fibrosis) was sufficient for abrogating fibrotic changes, likely via TRPA1 activation.

Previous studies have shown that TRPA1 participates in tissue inflammation and remodeling in various manners.¹⁵

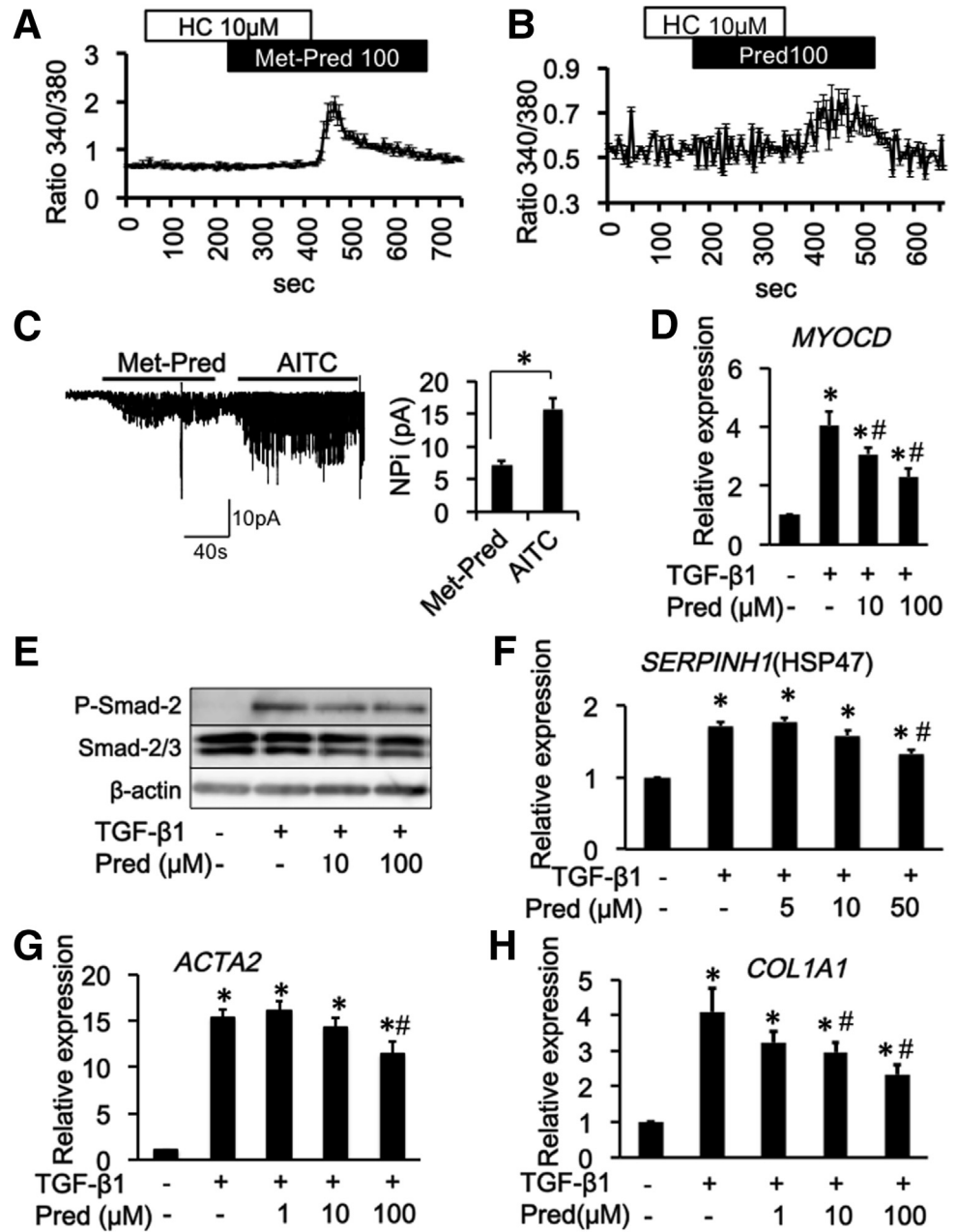


Figure 11. Steroids activate the TRPA1 channel and suppress TGF- β 1-induced fibrosis mediators in InMyoFibs. (A and B) Representative $[Ca^{2+}]_i$ responses in InMyoFibs cells. Cells were exposed to steroids, TRPA1 antagonist HC-030031 (10 μ mol/L) was added. Data points represent the means \pm SEM from > 30 cells. (C) Activated single-channel currents in TRPA1 expressed HEK293 cells. Representative traces of cell-attached recorded at a holding potential of -40 mV. The averaged density of single I_{TRPA1} at -40 mV (expressed as NPi) by application of Met-pred (100 μ mol/L) and AITC (10 μ mol/L) ($n = 6$). $P < .01$. (D-H) Prednisolone (Pred) was co-administered with TGF- β 1 in InMyoFib cells. (D) Myocardin (MYOCD) mRNA expression, (E) TGF- β 1-induced phosphorylation of Smad-2 was measured by Western blot, (F-H) HSP47 (SERPINH) and type 1 collagen (COL1A1), and α -SMA (ACTA2) mRNA expression measured by real-time PCR in InMyoFibs cells. * $P < .05$ vs control cells; # $P < .05$ vs TGF- β 1-treated cells ($n = 4$). Met-Pred, methylprednisolone.

TRPA1 is functional in both neuronal and non-neuronal cells to modulate local tissue inflammation in animal models of acute pulmonary inflammation induced by acrolein and cigarette smoke, experimental colitis, or carrageenan-induced paw edema.^{13,16,36} In mouse corneal stroma, TRPA1 is required for TGF- β signaling, and its genetic deletion abrogates inflammatory fibrosis.³⁷ Wound healing is a physiological process triggered by inflammation that may lead to tissue repair with reconstitution of normal morphology and function or fibrotic replacement depending on the balance between the production and degradation of extracellular matrix proteins.^{38,39} Thus, the negative regulation of intestinal TGF-receptor-mediated profibrotic signaling by myofibroblast TRPA1 identified in the present

study also may be involved in such multifaceted actions of TRPA1 in tissue inflammation/remodeling.

Steroids are widely used to treat fibrotic disorders. However, direct molecular targets of their antifibrotic effects remain unclear. The therapeutic concentrations of steroids for fibrotic diseases are thought to be much higher than those required to saturate the glucocorticoid receptors (genomic effects).⁴⁰ This raises the question of whether there is an additional target(s) for the non-genomic effects of glucocorticoids. The results of the present study clearly show that steroids (and pirfenidone) target TRPA1, the activation of which leads to the negative regulation of TGF- β 1-Smad signaling and eventually the down-regulation of antifibrotic factors such as collagen

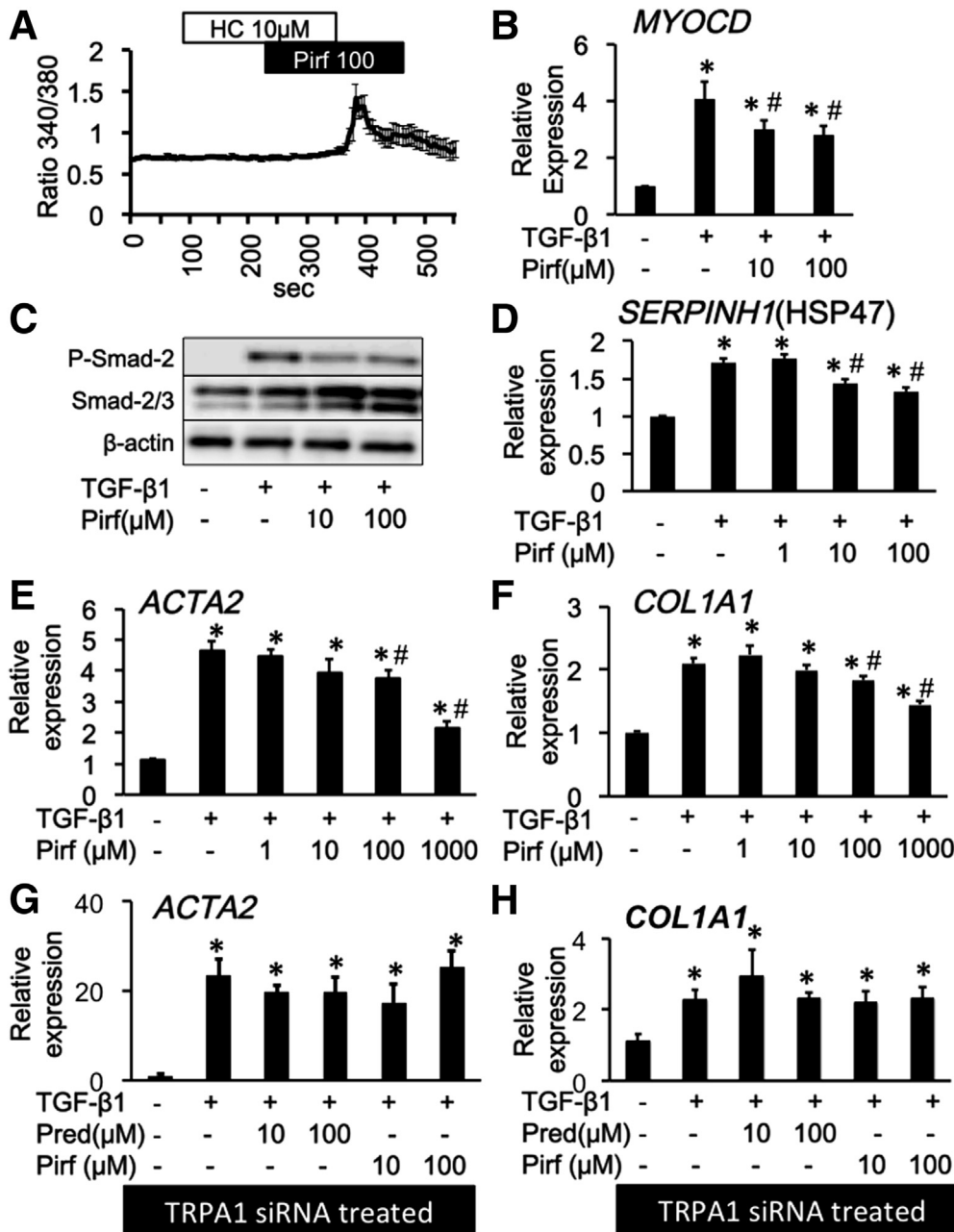


Figure 12. Pirfenidone activates the TRPA1 channel and suppresses TGF- β 1-induced fibrosis mediators in InMyoFibs. (A) Representative $[Ca^{2+}]_i$ responses in InMyoFib cells. Cells were exposed to pirfenidone (Pirf), TRPA1 antagonist HC-030031 (10 μ mol/L) was added. Data points represent the means \pm SEM from > 30 cells. (B–F) Pirfenidone was co-administered with TGF- β 1 in InMyoFib cells. (B) Myocardin (MYOCD) mRNA expression, (C) TGF- β 1-induced phosphorylation of Smad-2 was measured by Western blot, (D–F) HSP47 (SERPINH) and type 1 collagen (COL1A1) and α -SMA (ACTA2) mRNA expression measured by real-time PCR in InMyoFib cells. * P < .05 vs control cells; # P < .05 vs TGF- β 1-treated cells (n = 4). (G–H) Type 1 collagen (COL1A1) and α -SMA (ACTA2) mRNA expression measured by real-time PCR in TRPA1 siRNA-pretreated InMyoFib cells. * P < .05 vs TRPA1 siRNA-treated control cells.

type I and α -SMA (Figures 9, 10, 11, and 12). However, our previous study showed that activation of the myofibroblast TRPC6 channel also can suppress fibrotic changes by inhibiting TGF- β 1–Smad signaling via the calcineurin-mediated pathway.³ This raises the question of whether TRPA1 and TRPC6 mediate myofibroblast fibrotic signaling in a redundant manner. However, the process mediated by TRPC6 requires a longer time than TRPA1 because the former is critically dependent on up-regulation of TRPC6 expression by TGF- β 1.³ In contrast, the TRPA1 channel is constitutively active in the gut and further up-regulated by TGF- β 1 stimulation. This indicates that targeting of the TRPA1 channel may be prophylactic against and/or beneficial in an earlier stage of inflammatory fibrosis as

compared with TRPC6. According to the recent study of TRPA1 structure, the pre-S1 region of N-terminal domain would be suited to detect reactive chemical agonists and interact with the TRP-like domain causing allosteric modulation. Thus, through a similar mechanism, steroid may induce a conformational change of TRPA1 channel leading to channel opening.

The higher prevalence of fibrosis in CD is likely the consequence of transmural bowel inflammation that exposes all mesenchymal cells capable of producing the extracellular matrix to fibrotic mediators.⁴¹ The findings from stenotic and nonstenotic biopsy samples suggest that the same mechanism as that involved in InMyoFib may operate in the stenotic lesion of intestines from CD

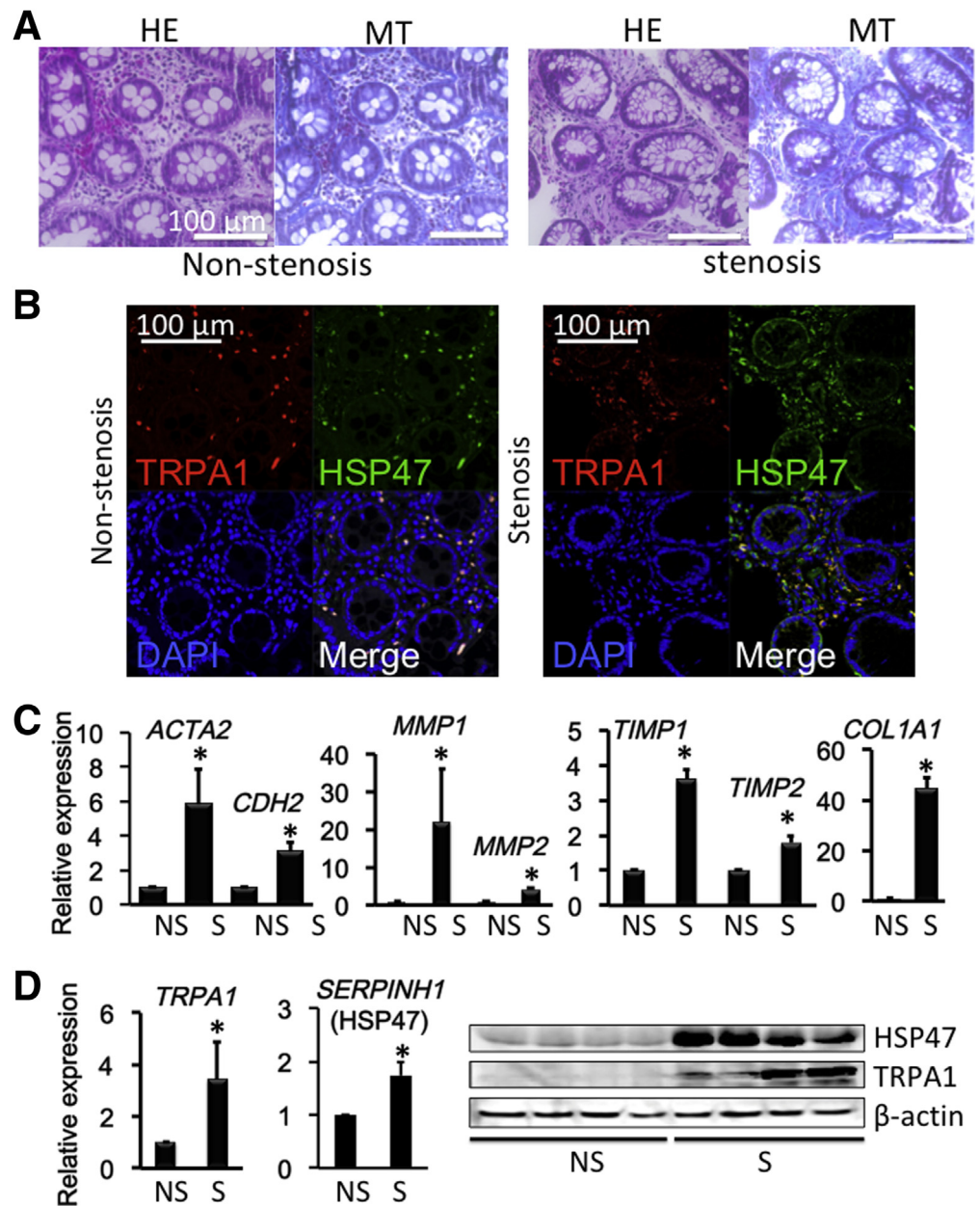


Figure 13. Colonoscopy and biopsy sampling was performed and showed a fibrotic lesion responsible for colon stenosis. (A) H&E-stained and MT-stained CD patient biopsy specimens of nonstenotic or stenotic intestinal areas. (B) Immunostaining of TRPA1/HSP47 in non-stenosis and stenosis biopsy samples. (C) mRNA levels ($n = 8$) of *ACTA2* (α -SMA), *CDH2* (N-cadherin), *MMP1*, *MMP2*, tissue inhibitor of metalloproteinase 1 (*TIMP1*), *TIMP2*, and *COL1A1* mRNA in biopsy specimens were examined by real-time RT-PCR in nonstenotic or stenotic inflamed mucosal tissues of CD patients. (D) *TRPA1* and *HSP47* mRNA ($n = 8$) and protein ($n = 4$) levels were examined in non-stenotic or stenotic inflamed mucosal tissues of CD patients. * $P < .05$ vs nonstenotic sample (16 paired samples obtained from 8 patients). DAPI, 4',6-diamidino-2-phenylindole.

patients. Of the 8 CD patients with stenotic lesions investigated in the present study, 7 patients already received anti-tumor necrosis factor (TNF) therapy. Although steroids and pirfenidone should be the first-line therapy in patients with mild-to-moderate CD without poor prognostic factors or complicated disease, anti-TNF treatment is regarded as a better choice for CD patients with complications or bowel damage with poor prognostic factors and/or severe disease.⁴² However, anti-TNF treatment may worsen stenotic fibrosis because rapid mucosal healing induced by TNF α antibody may facilitate excessive fibrosis.⁴³ Therefore, therapeutic strategies that distinguish between these states may yield more beneficial outcomes than currently available therapeutic regimens. For instance, topical administration of steroid is used as an

initial treatment for CD.^{44,45} Our finding that myofibroblast TRPA1 contributes to intestinal fibrosis is of great therapeutic significance, and may be generalized to other fibrotic lesions such as those in the skin, lung, and liver, where several TRP channels, including TRPA1, are highly expressed. In addition, the collagen-specific molecular chaperone HSP47, which was co-expressed with TRPA1 in the present study, is a stress-inducible protein up-regulated by heat, shear stress, oxidation, and other stimuli, and thus is another candidate molecule related to intestinal fibrosis in CD. This raises another intriguing question that should be addressed in future studies: whether and how these molecules functionally interact to contribute to the pathogenesis of fibrotic complications of inflammatory bowel disease.

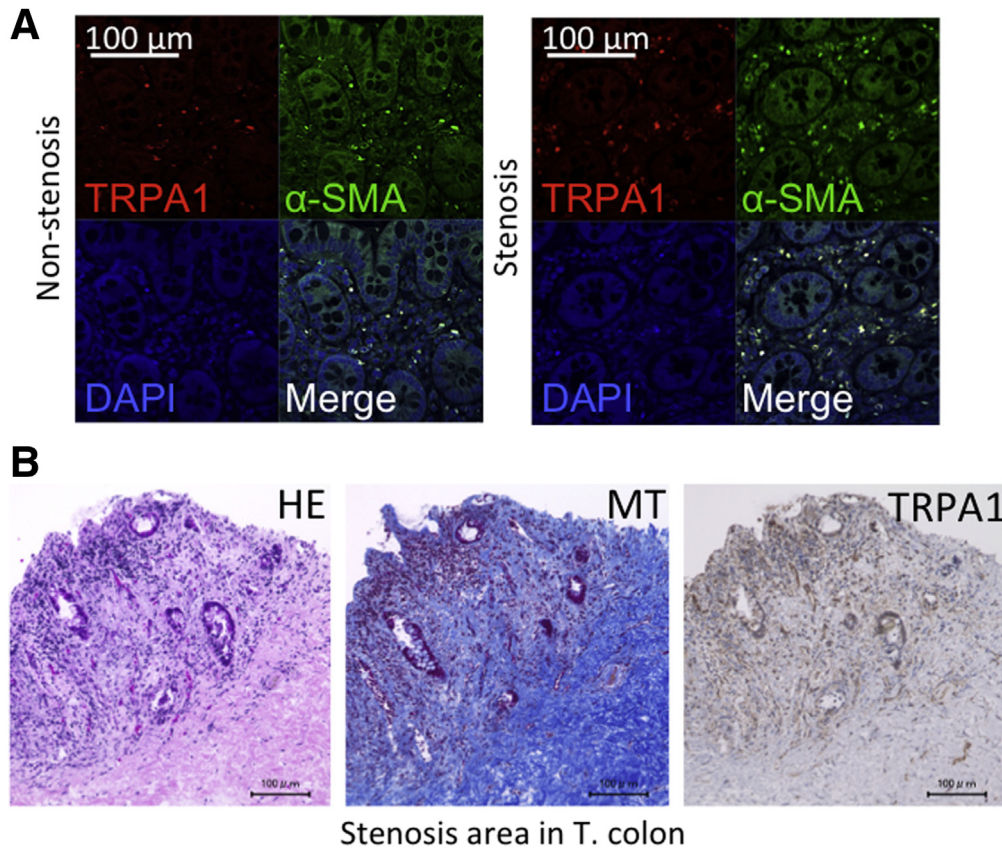


Figure 14. TRPA1 localization in CD patient intestine. (A) Immunostaining of TRPA1/ α -SMA in nonstenosis and stenosis biopsy samples. (B) H&E-, MT-, and TRPA1-3,3'-diaminobenzidine tetrahydrochloride (DAB)-stained stenosis surgical tissue from a CD patient transverse colon. DAPI, 4',6'-diamidino-2-phenylindole. T. colon, transverse colon.

In summary, the present study showed a new role for the myofibroblast TRPA1 channel in intestinal fibrosis and that steroids and pirfenidone activate this channel to exert its antifibrotic effects. Identification of this new antifibrotic molecular target TRPA1 will lead to additional studies of the pharmacologic actions of steroids and pirfenidone, as well as improve our understanding of the additive/synergistic effects and side effects of distinct antifibrotic drugs. The present findings not only provide a novel molecular target for antifibrotic therapy of inflammatory bowel diseases, but also a framework for re-interpreting the theory of inflammation and fibrosis in the gut.

References

- Rieder F, Brenmoehl J, Leeb S, Scholmerich J, Rogler G. Wound healing and fibrosis in intestinal disease. *Gut* 2007;56:130–139.
- Hinz B. Formation and function of the myofibroblast during tissue repair. *J Invest Dermatol* 2007;127:526–537.
- Kurahara LH, Sumiyoshi M, Aoyagi K, Hiraishi K, Nakajima K, Nakagawa M, Hu Y, Inoue R. Intestinal myofibroblast TRPC6 channel may contribute to stenotic fibrosis in Crohn's disease. *Inflamm Bowel Dis* 2015; 21:496–506.
- Medina C, Santos-Martinez MJ, Santana A, Paz-Cabrera MC, Johnston MJ, Mourelle M, Salas A, Guarner F. Transforming growth factor-beta type 1 receptor (ALK5) and Smad proteins mediate TIMP-1 and collagen synthesis in experimental intestinal fibrosis. *J Pathol* 2011;224:461–472.
- Inoue K, Naito Y, Takagi T, Hayashi N, Hirai Y, Mizushima K, Horie R, Fukumoto K, Yamada S, Harusato A, Hirata I, Omatsu T, Yoshida N, Uchiyama K, Ishikawa T, Handa O, Konishi H, Wakabayashi N, Yagi N, Ichikawa H, Kokura S, Yoshikawa T. Daikenchuto, a Kampo medicine, regulates intestinal fibrosis associated with decreasing expression of heat shock protein 47 and collagen content in a rat colitis model. *Biol Pharm Bull* 2011;34:1659–1665.
- Kitamura H, Yamamoto S, Nakase H, Matsuura M, Honzawa Y, Matsumura K, Takeda Y, Uza N, Nagata K, Chiba T. Role of heat shock protein 47 in intestinal fibrosis of experimental colitis. *Biochem Biophys Res Commun* 2011;404:599–604.
- Johnson LA, Rodansky ES, Haak AJ, Larsen SD, Neubig RR, Higgins PD. Novel Rho/MRTF/SRF inhibitors block matrix-stiffness and TGF-beta-induced fibrogenesis in human colonic myofibroblasts. *Inflamm Bowel Dis* 2014;20:154–165.
- Babyatsky MW, Rossiter G, Podolsky DK. Expression of transforming growth factors alpha and beta in colonic mucosa in inflammatory bowel disease. *Gastroenterology* 1996;110:975–984.
- Inoue R, Jensen LJ, Shi J, Morita H, Nishida M, Honda A, Ito Y. Transient receptor potential channels in cardiovascular function and disease. *Circ Res* 2006; 99:119–131.

10. Nishida M, Onohara N, Sato Y, Suda R, Ogushi M, Tanabe S, Inoue R, Mori Y, Kurose H. α 12/13-mediated up-regulation of TRPC6 negatively regulates endothelin-1-induced cardiac myofibroblast formation and collagen synthesis through nuclear factor of activated T cells activation. *J Biol Chem* 2007;282:23117–23128.
11. Onohara N, Nishida M, Inoue R, Kobayashi H, Sumimoto H, Sato Y, Mori Y, Nagao T, Kurose H. TRPC3 and TRPC6 are essential for angiotensin II-induced cardiac hypertrophy. *EMBO J* 2006;25:5305–5316.
12. Du J, Xie J, Zhang Z, Tsujikawa H, Fusco D, Silverman D, Liang B, Yue L. TRPM7-mediated Ca^{2+} signals confer fibrogenesis in human atrial fibrillation. *Circ Res* 2010;106:992–1003.
13. Poole DP, Pelayo JC, Cattaruzza F, Kuo YM, Gai G, Chiu JV, Bron R, Furness JB, Grady EF, Bunnett NW. Transient receptor potential ankyrin 1 is expressed by inhibitory motoneurons of the mouse intestine. *Gastroenterology* 2011;141:565–575 e561–e564.
14. Kono T, Kaneko A, Omiya Y, Ohbuchi K, Ohno N, Yamamoto M. Epithelial transient receptor potential ankyrin 1 (TRPA1)-dependent adrenomedullin upregulates blood flow in rat small intestine. *Am J Physiol Gastrointest Liver Physiol* 2013;304:G428–G436.
15. Bautista DM, Pellegrino M, Tsunozaki M. TRPA1: a gatekeeper for inflammation. *Annu Rev Physiol* 2013;75:181–200.
16. Nassini R, Pedretti P, Moretto N, Fusi C, Carnini C, Facchinetti F, Viscomi AR, Pisano AR, Stokesberry S, Brunmark C, Svitacheva N, McGarvey L, Patacchini R, Damholt AB, Geppetti P, Materazzi S. Transient receptor potential ankyrin 1 channel localized to non-neuronal airway cells promotes non-neurogenic inflammation. *PLoS One* 2012;7:e42454.
17. Lee BH, Hsu WH, Hsu YW, Pan TM. Suppression of dimeric acid on hepatic fibrosis caused from carboxymethyl-lysine (CML) by attenuating oxidative stress depends on Nrf2 activation in hepatic stellate cells (HSCs). *Food Chem Toxicol* 2013;62:413–419.
18. Jiang X, Zhang Y, Li F, Zhu Y, Chen Y, Yang S, Sun G. Allicin as a possible adjunctive therapeutic drug for stage II oral submucous fibrosis: a preliminary clinical trial in a Chinese cohort. *Int J Oral Maxillofac Surg* 2015;44:1540–1546.
19. Kun J, Szitter I, Kemeny A, Perkecz A, Kereskai L, Pohoczky K, Vincze A, Godi S, Szabo I, Szolcsanyi J, Pinter E, Helyes Z. Upregulation of the transient receptor potential ankyrin 1 ion channel in the inflamed human and mouse colon and its protective roles. *PLoS One* 2014;9:e108164.
20. Bertin S, Aoki-Nonaka Y, Lee J, de Jong PR, Kim P, Han T, Yu T, To K, Takahashi N, Boland BS, Chang JT, Ho SB, Herdman S, Corr M, Franco A, Sharma S, Dong H, Akopian AN, Raz E. The TRPA1 ion channel is expressed in CD4^{+} T cells and restrains T-cell-mediated colitis through inhibition of TRPV1. *Gut* 2017;66:1584–1596.
21. Romano B, Borrelli F, Fasolino I, Capasso R, Piscitelli F, Cascio M, Pertwee R, Coppola D, Vassallo L, Orlando P, Di Marzo V, Izzo A. The cannabinoid TRPA1 agonist cannabichromene inhibits nitric oxide production in macrophages and ameliorates murine colitis. *Br J Pharmacol* 2013;169:213–229.
22. Brooker JC, Beckett CG, Saunders BP, Benson MJ. Long-acting steroid injection after endoscopic dilation of anastomotic Crohn's strictures may improve the outcome: a retrospective case series. *Endoscopy* 2003;35:333–337.
23. Van Assche G. Intramural steroid injection and endoscopic dilation for Crohn's disease. *Clin Gastroenterol Hepatol* 2007;5:1027–1028.
24. Meier R, Lutz C, Cosin-Roger J, Fagagnini S, Bollmann G, Hunerwadel A, Mamie C, Lang S, Tchouboukov A, Weber FE, Weber A, Rogler G, Hausmann M. Decreased fibrogenesis after treatment with pirfenidone in a newly developed mouse model of intestinal fibrosis. *Inflamm Bowel Dis* 2016;22:569–582.
25. Inoue YN, Takagi T, Hayashi N, Hirai Y, Mizushima K, Tsuji T, Yoriki H, Kugai M, Horie R, Fukumoto K, Yamada S, Harusato A, Yoshida N, Uchiyama K, Ishikawa T, Handa O, Konishi H, Wakabayashi N, Yagi N, Ichikawa H, Kokura S, Yoshikawa T. Pirfenidone regulates intestinal fibrosis through the inhibition of HSP47 expression in a rat colitis model. *Gastroenterology* 2011;140(Suppl 1):S-770.
26. Honzawa Y, Nakase H, Takeda Y, Nagata K, Chiba T. Heat shock protein 47 can be a new target molecule for intestinal fibrosis related to inflammatory bowel disease. *Inflamm Bowel Dis* 2010;16:2004–2006.
27. Nakase H, Honzawa Y, Chiba T. Heat shock protein 47 is a new candidate molecule as anti-fibrotic treatment of Crohn's disease. *Aliment Pharmacol Ther* 2010;31:926–928.
28. Shi J, Mori E, Mori Y, Mori M, Li J, Ito Y, Inoue R. Multiple regulation by calcium of murine homologues of transient receptor potential proteins TRPC6 and TRPC7 expressed in HEK293 cells. *J Physiol* 2004;561:415–432.
29. Takahashi N, Kuwaki T, Kiyonaka S, Numata T, Kozai D, Mizuno Y, Yamamoto S, Naito S, Knevels E, Carmeliet P, Oga T, Kaneko S, Suga S, Nokami T, Yoshida J, Mori Y. TRPA1 underlies a sensing mechanism for O_2 . *Nat Chem Biol* 2011;7:701–711.
30. Fujihara Y, Ikawa M. CRISPR/Cas9-based genome editing in mice by single plasmid injection. *Methods Enzymol* 2014;546:319–336.
31. Mashiko D, Fujihara Y, Satouh Y, Miyata H, Isotani A, Ikawa M. Generation of mutant mice by pronuclear injection of circular plasmid expressing Cas9 and single guided RNA. *Sci Rep* 2013;3:3355.
32. Johnson LA, Luke A, Sauder K, Moons DS, Horowitz JC, Higgins PD. Intestinal fibrosis is reduced by early elimination of inflammation in a mouse model of IBD: impact of a "Top-Down" approach to intestinal fibrosis in mice. *Inflamm Bowel Dis* 2012;18:460–471.
33. Fichtner-Feigl S, Fuss IJ, Young CA, Watanabe T, Geissler EK, Schlitt HJ, Kitani A, Strober W. Induction of IL-13 triggers TGF- β 1-dependent tissue fibrosis in chronic 2,4,6-trinitrobenzene sulfonic acid colitis. *J Immunol* 2007;178:5859–5870.

34. Rieder F, Fiocchi C, Rogler G. Mechanisms, management, and treatment of fibrosis in patients with inflammatory bowel diseases. *Gastroenterology* 2017;152:340–350 e346.
35. Hinz B, Gabbiani G. Fibrosis: recent advances in myofibroblast biology and new therapeutic perspectives. *F1000 Biol Rep* 2010;2:78.
36. Moilanen LJ, Laavola M, Kukkonen M, Korhonen R, Leppanen T, Hogestatt ED, Zygmunt PM, Nieminen RM, Moilanen E. TRPA1 contributes to the acute inflammatory response and mediates carrageenan-induced paw edema in the mouse. *Sci Rep* 2012;2:380.
37. Okada Y, Shirai K, Reinach PS, Kitano-Izutani A, Miyajima M, Flanders KC, Jester JV, Tominaga M, Saika S. TRPA1 is required for TGF-beta signaling and its loss blocks inflammatory fibrosis in mouse corneal stroma. *Lab Invest* 2014;94:1030–1041.
38. Specia S, Giusti I, Rieder F, Latella G. Cellular and molecular mechanisms of intestinal fibrosis. *World J Gastroenterol* 2012;18:3635–3661.
39. Latella G, Di Gregorio J, Flati V, Rieder F, Lawrance IC. Mechanisms of initiation and progression of intestinal fibrosis in IBD. *Scand J Gastroenterol* 2015;50:53–65.
40. Adcock IM, Nasuhara Y, Stevens DA, Barnes PJ. Ligand-induced differentiation of glucocorticoid receptor (GR) trans-repression and transactivation: preferential targeting of NF-kappaB and lack of I-kappaB involvement. *Br J Pharmacol* 1999;127:1003–1011.
41. Latella G, Sferra R, Specia S, Vetuschi A, Gaudio E. Can we prevent, reduce or reverse intestinal fibrosis in IBD? *Eur Rev Med Pharmacol Sci* 2013;17:1283–1304.
42. Peyrin-Biroulet L, Fiorino G, Buisson A, Danese S. First-line therapy in adult Crohn's disease: who should receive anti-TNF agents? *Nat Rev Gastroenterol Hepatol* 2013;10:345–351.
43. Condino G, Calabrese E, Zorzi F, Onali S, Lolli E, De Biasio F, Ascolani M, Pallone F, Biancone L. Anti-TNF-alpha treatments and obstructive symptoms in Crohn's disease: a prospective study. *Dig Liver Dis* 2013;45:258–262.
44. Kuenzig ME, Rezaie A, Seow CH, Otlej AR, Steinhart AH, Griffiths AM, Kaplan GG, Benchimol EI. Budesonide for maintenance of remission in Crohn's disease. *Cochrane Database Syst Rev* 2014;8:CD002913.
45. Coward S, Kuenzig ME, Hazlewood G, Clement F, McBrien K, Holmes R, Panaccione R, Ghosh S, Seow CH, Rezaie A, Kaplan GG. Comparative effectiveness of mesalamine, sulfasalazine, corticosteroids, and budesonide for the induction of remission in Crohn's disease: a Bayesian network meta-analysis. *Inflamm Bowel Dis* 2017;23:461–472.

Received July 2, 2017. Accepted December 7, 2017.

Correspondence

Address correspondence to: Lin Hai Kurahara, PhD, Department of Physiology, Faculty of Medicine, Fukuoka University, Fukuoka 814-0180, Japan. e-mail: haiilin@fukuoka-u.ac.jp; fax: (81) 92-865-6032.

Acknowledgments

The authors thank NPO Biotechnology Research and Development for technical assistance. The authors thank the Biotechnology and Food Research Institute, Fukuoka Industrial Technology Centre, for providing the 103 herb library for screening; Professor Keichiro Haga coordinated this collaboration. The authors thank Professor Yasuo Mori (Kyoto University, Japan), who kindly provided TRPA1 plasmids. The authors also would like to thank Editage (www.editage.jp) for English language editing. The authors thank cell-innovator supported Microarray analysis.

Author contributions

Lin Hai Kurahara designed the experiments and wrote the paper; Lin Hai Kurahara and Keizo Hiraishi performed most experiments and analyzed the data; Yaopeng Hu conducted patch clamp experiments and analyzed the obtained data; Kaori Koga and Miki Onitsuka performed pathologic analysis; Mayumi Doi and Yuwen Jian performed immunostaining experiments and collected data; Kunihiro Aoyagi, Hidetoshi Takedatsu, and Daibo Kojima gave clinical advice, recruited study participants, performed biopsies, and surgically resected tissues; Yoshitaka Fujihara generated *Trpa1* knockout mice with the Clustered regularly interspaced short palindromic repeats (CRISPR)/CRISPR-associated 9 (Cas9) system; Yuwen Jian created a graphical abstract; and Ryuji Inoue supervised the study and provided comments during the preparation of this manuscript.

Conflicts of interest

The authors disclose no conflicts.

Funding

This study was supported by The Ministry of Education, Culture, Sports, Science and Technology (MEXT) KAKENHI (15K08978, 22790677, and 25860571); the Fukuoka Foundation for Sound Health Cancer Research Fund; the MEXT-Supported Program supporting the research activities of female researchers; the Clinical Research Foundation; and the Central Research Institute of Fukuoka University (151045 and 147104).